A tutorial overview of
forward-inverse modeling based on AccuRT

FIRST: Water BRDF Study

Correcting bidirectional effects in remote sensing reflectance from coastal waters

Yongzhen Fan[a], Zhenyi Lin[a], Wei Li[a],
Charles Gatebe[b,c], Kenneth Voss[d], Knut Stamnes[a]

[a]Light and Life Laboratory
Department of Physics
Stevens Institute of Technology
Hoboken, New Jersey, USA

[b]NASA Goddard Space Flight Center, Greenbelt, Maryland, USA

[c]Universities Space Research Association, Columbia, Maryland, USA

[d]Department of Physics, University of Miami, Miami, Florida, USA

For details see: Fan, Yongzhen, Li, Wei, Voss, Kenneth J, Gatebe, Charles K, and Stamnes, Knut. Neural network method to correct bidirectional effects in water-leaving radiance. Applied Optics, 55, 10-21, 2016.

Why are bidirectional effects important?

The Bidirectional Reflectance Distribution Function (BRDF) is defined as the ratio of the reflected radiance to the incident power per unit surface area:

$$\rho(\mu, \phi; -\mu', \phi') = \frac{dI_{\text{refl}}(\tau^*, \mu, \phi)}{I(\tau^*, -\mu', \phi')\ \mu'\ d\mu' d\phi'} \tag{1}$$

where $dI_{\text{refl}}(\tau^*, \mu, \phi)$ is the reflected radiance in direction (μ, ϕ), while $I(\tau^*, -\mu', \phi')$ is the incident radiance in direction $(-\mu', \phi')$.

Understanding bidirectional effects including sunglint is important for several reasons:

1. **Correct interpretation of ocean color data.**
2. **Comparing consistency of spectral radiance data derived from space observations with a single instrument for a variety of illumination and viewing conditions.**
3. **Merging data collected by different instruments operating simultaneously.**

We present a new neural network method to correct for bidirectional effects in water-leaving radiances for both clear and turbid (coastal) waters.

Light and Life Laboratory STEVENS Institute of Technology

Bidirectional effect in oceanic water

The water-leaving radiance (L_{w}) or remote sensing reflectance ($R_{\mathrm{rs}} \propto L_{\mathrm{w}}$) depends on:

- Illumination conditions at the ocean surface
- Optical properties of the water, especially of embedded particles
- Sun-sensor geometry (i.e. solar zenith angle θ_0, sensor zenith angle θ, and relative azimuth angle $\Delta\phi$).

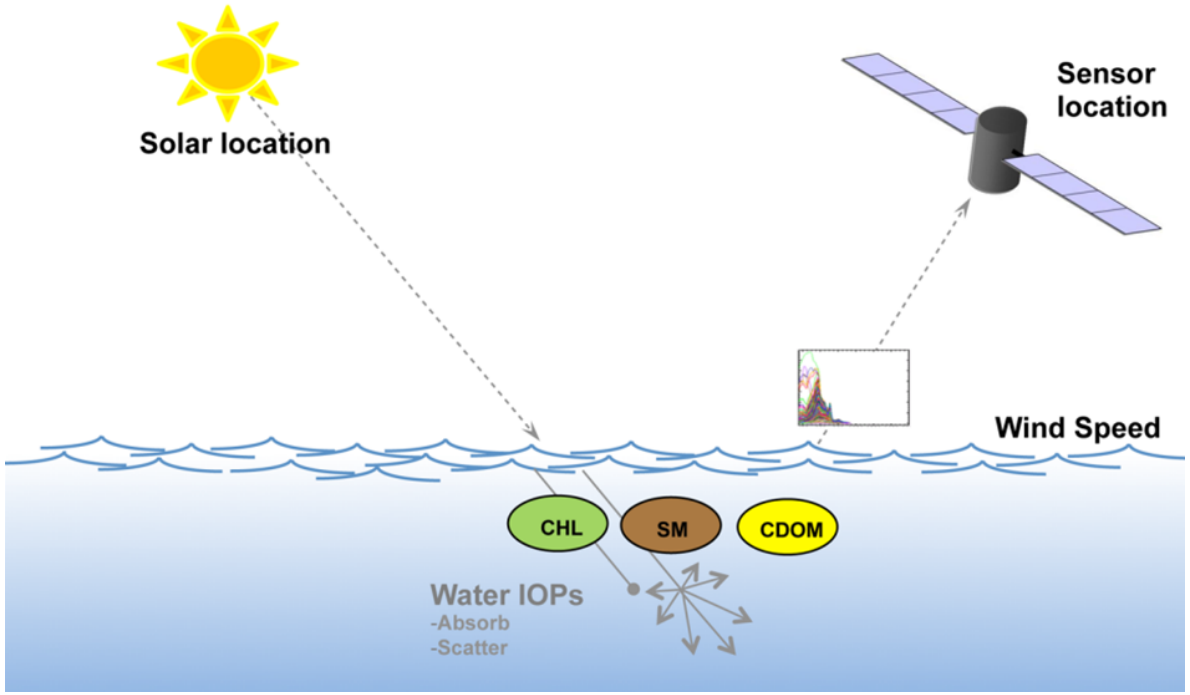

Light and Life Laboratory STEVENS Institute of Technology

Current BRDF correction algorithms

A BRDF correction algorithm was developed by Morel, Antoine and Gentili in 2002 (denoted as MAG02) based on the following expression for the normalized water-leaving radiance $nL_{\rm w}$:

$$nL_{\rm w} = L_{\rm w} \times \frac{\Re_{\rm o}}{\Re} \times \frac{f_0(\tau_a, W, IOP)}{Q_0(\tau_a, W, IOP)} \times \left[\frac{f(\theta_0, \theta, \Delta\phi, \tau_a, W, IOP)}{Q(\theta_0, \theta, \Delta\phi, \tau_a, W, IOP)}\right]^{-1}$$

However, the MAG02 algorithm:

- requires CHL to derive the f/Q correction factor
- does not work well in turbid (coastal) waters.

Our simulations show that:

- Differences in spectral $R_{\rm rs}$ values are significant between clear (open ocean) and turbid (coastal) waters,
- but very small between nadir- and slant-viewing directions for a given water type.

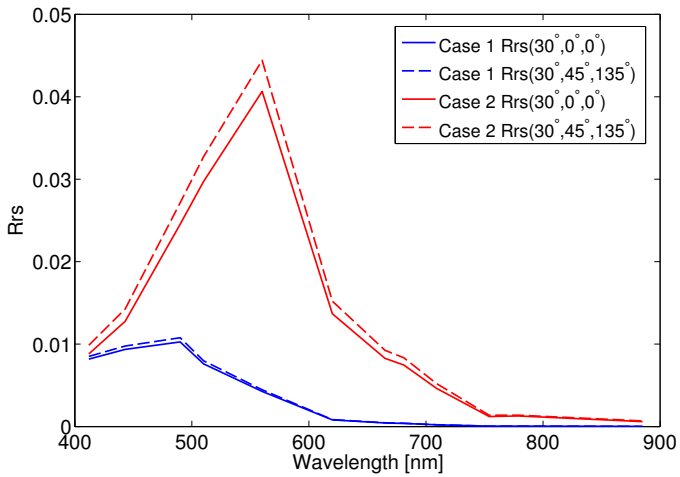

Light and Life Laboratory — STEVENS Institute of Technology

Neural Network BRDF correction algorithm

- A trained Radial Basis Function Neural Network (RBF-NN) can convert the spectral $R_{\rm rs}$ from the slant- to the nadir-viewing direction:

$$R_{\rm rs}(\lambda_i,\theta_0) = \sum_{j=1}^{N_{neu}} a_{ij} \times \exp\left[- b^2 \sum_{k=1}^{N_{input}} [R_{rs}(\lambda_k,\theta_0,\theta,\Delta\phi) - c_{jk}]^2 \right] + d_i$$

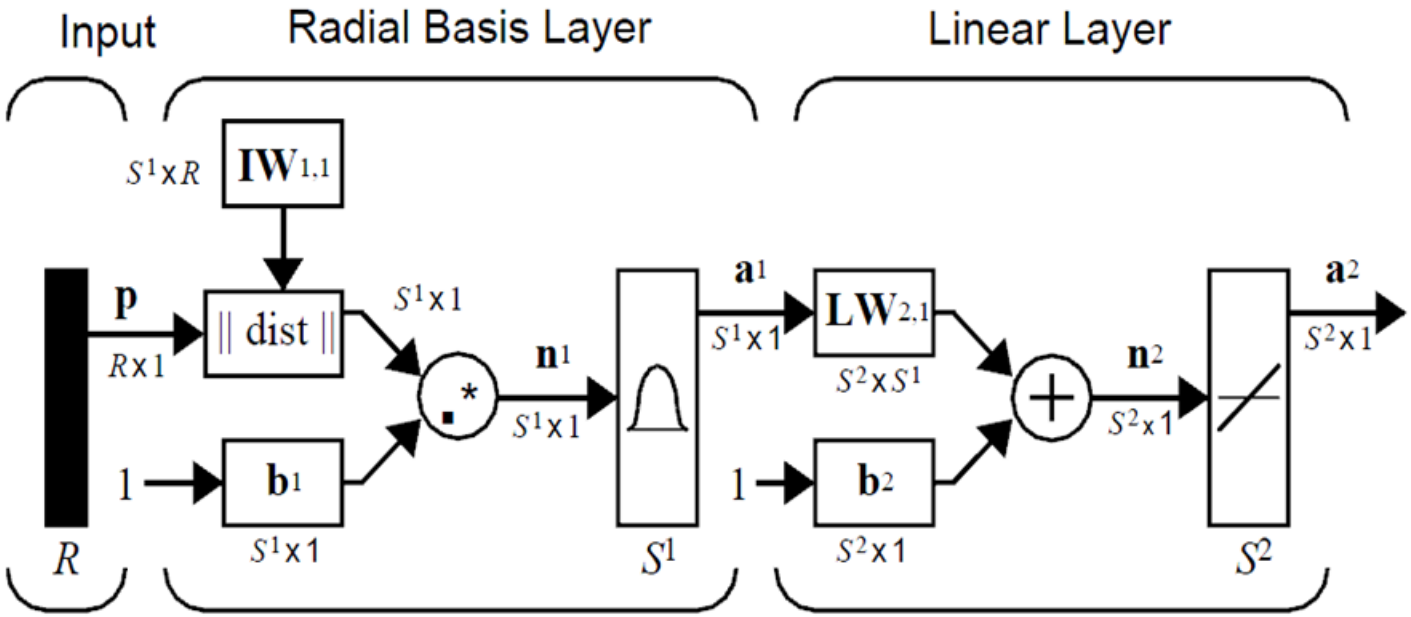

Remote sensing reflectance simulation

- Simulate R_{rs} at both nadir- and slant-viewing directions (AccuRT)

$$R_{\rm rs}(\lambda,\theta_0,\theta,\Delta\phi) = \left[L_u^{0+} - L_{u,\rm blk\_oc}^{0+}(\lambda,\theta_0,\theta,\Delta\phi)\right]/E_d^{0+}(\lambda)$$

- Radiative transfer model setup
  - 13 layers U.S. standard atmosphere with aerosols added in the bottom 0-2 km.
  - randomly selected aerosol models based on fraction of small-mode aerosol particles (f) and relative humidity (RH).
  - CCRR bio-optical model parameterized in terms of CHL, CDOM and MIN.
    - $a_{\rm CHL}(\lambda) = A(\lambda) \times {\rm CHL}^{E(\lambda)}$
    - $b_{\rm CHL}(\lambda) = 0.407 \times {\rm CHL}^{0.795} \times (\lambda/660)^{\nu} - a_{\rm CHL}(\lambda)$
    - $a_{\rm CDOM}(\lambda) = {\rm CDOM} \times \exp\left[-0.0176(\lambda - 443)\right]$
    - $a_{\rm MIN}(\lambda) = 0.031 \times {\rm MIN} \times \exp\left[-0.0123(\lambda - 443)\right]$
    - $b_{\rm MIN}(\lambda) = 0.518 \times {\rm MIN} \times (\lambda/555)^{-0.3749} - a_{\rm MIN}(\lambda)$

Light and Life Laboratory STEVENS Institute of Technology

Neural network method validation – synthetic data

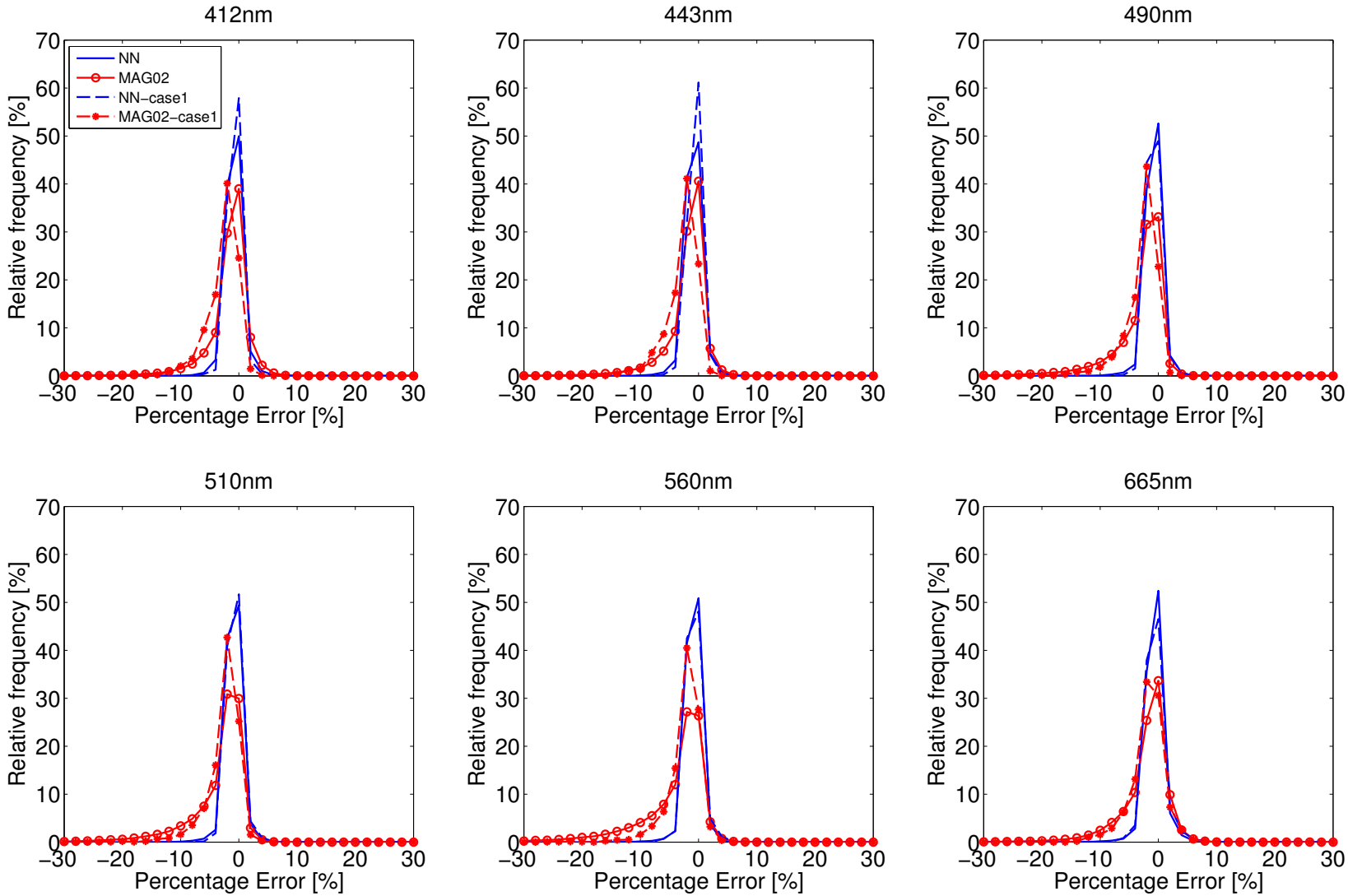

Comparison between MAG02 and RBF-NN method using synthetic dataset.

Light and Life Laboratory STEVENS Institute of Technology

Neural network method validation – NuRADS data

NuRADS is a compact camera system that takes images of the upward radiance just below the ocean surface at various geometry angles and multiple wavelengths centered at 411, 436, 487, 526, 548 and 616 nm.

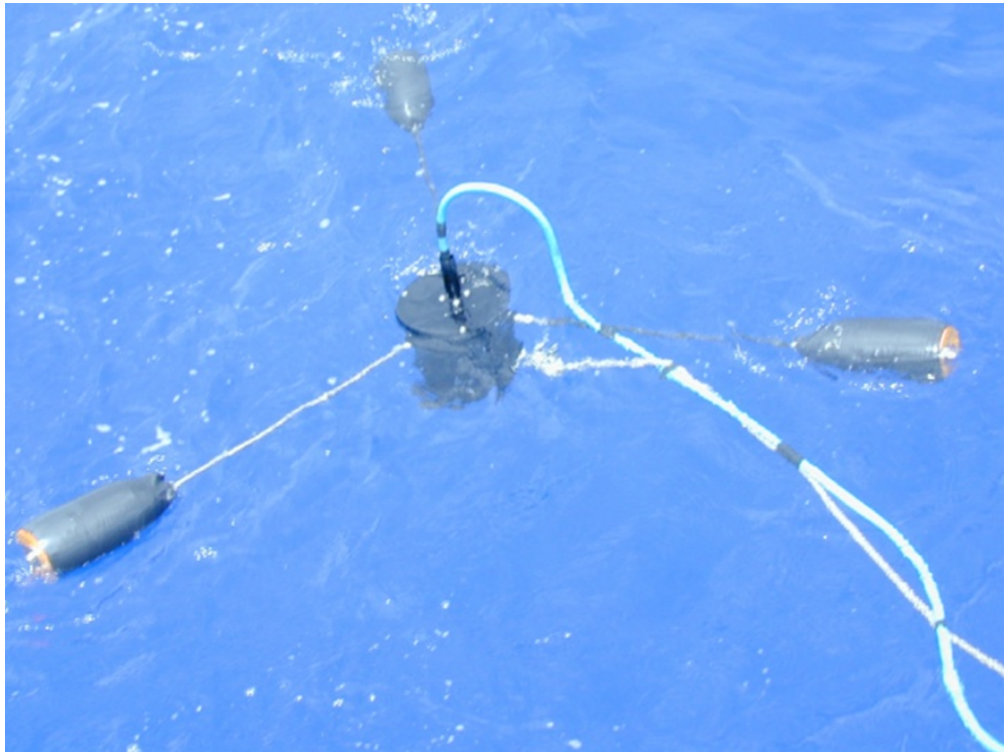

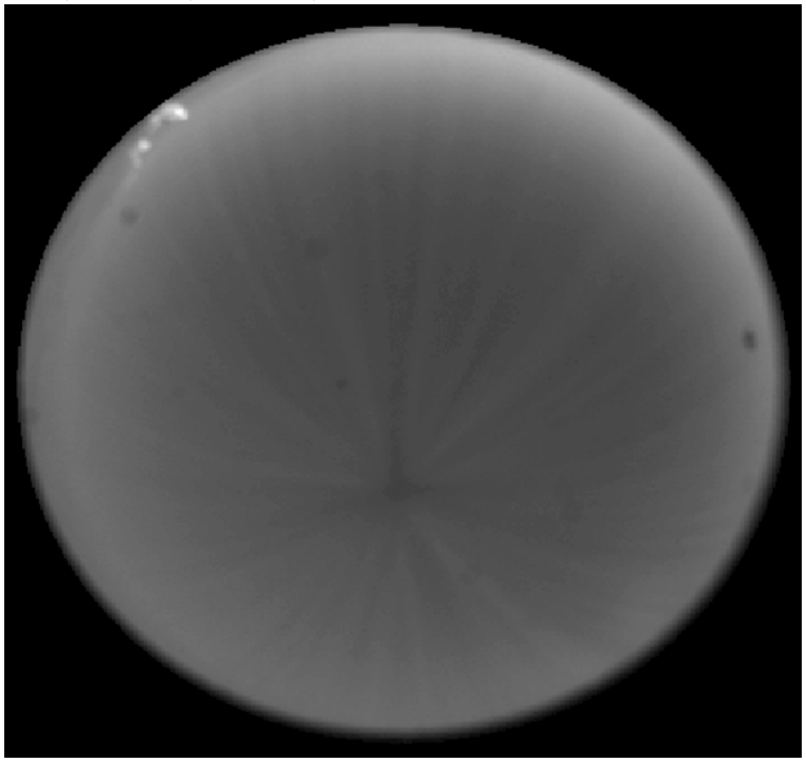

Light and Life Laboratory STEVENS Institute of Technology

Neural network method validation – NuRADS data

- The NuRADS system was used in many field experiments and a large quantity of *in-situ* data is available in NASA's SeaBASS validation data base.

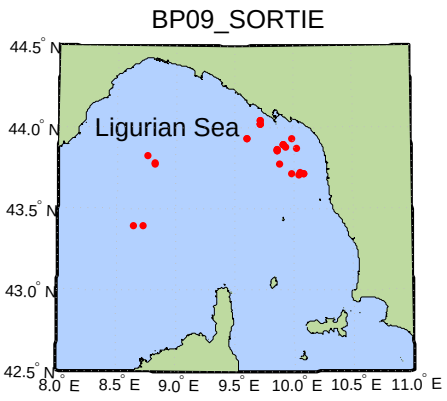

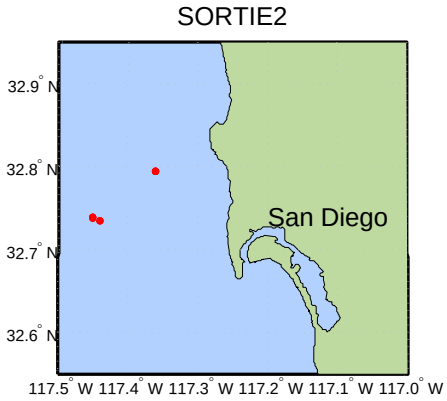

- BP09: March, 2008. N = 28
- SORTIE2: Jan., 2008. N = 13
- BIOSOPE: Oct., 2004. N = 11
- OCCV : May, 2009. N = 7

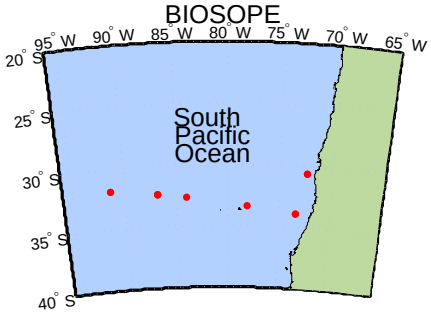

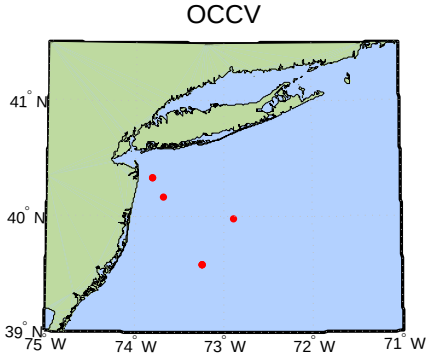

- Geometry range:
  - θ: 0° – 45° with 5° intervals
  - $\Delta\phi$: 0° – 180° with 10° intervals

Light and Life Laboratory STEVENS Institute of Technology

Neural network method validation – NuRADS data

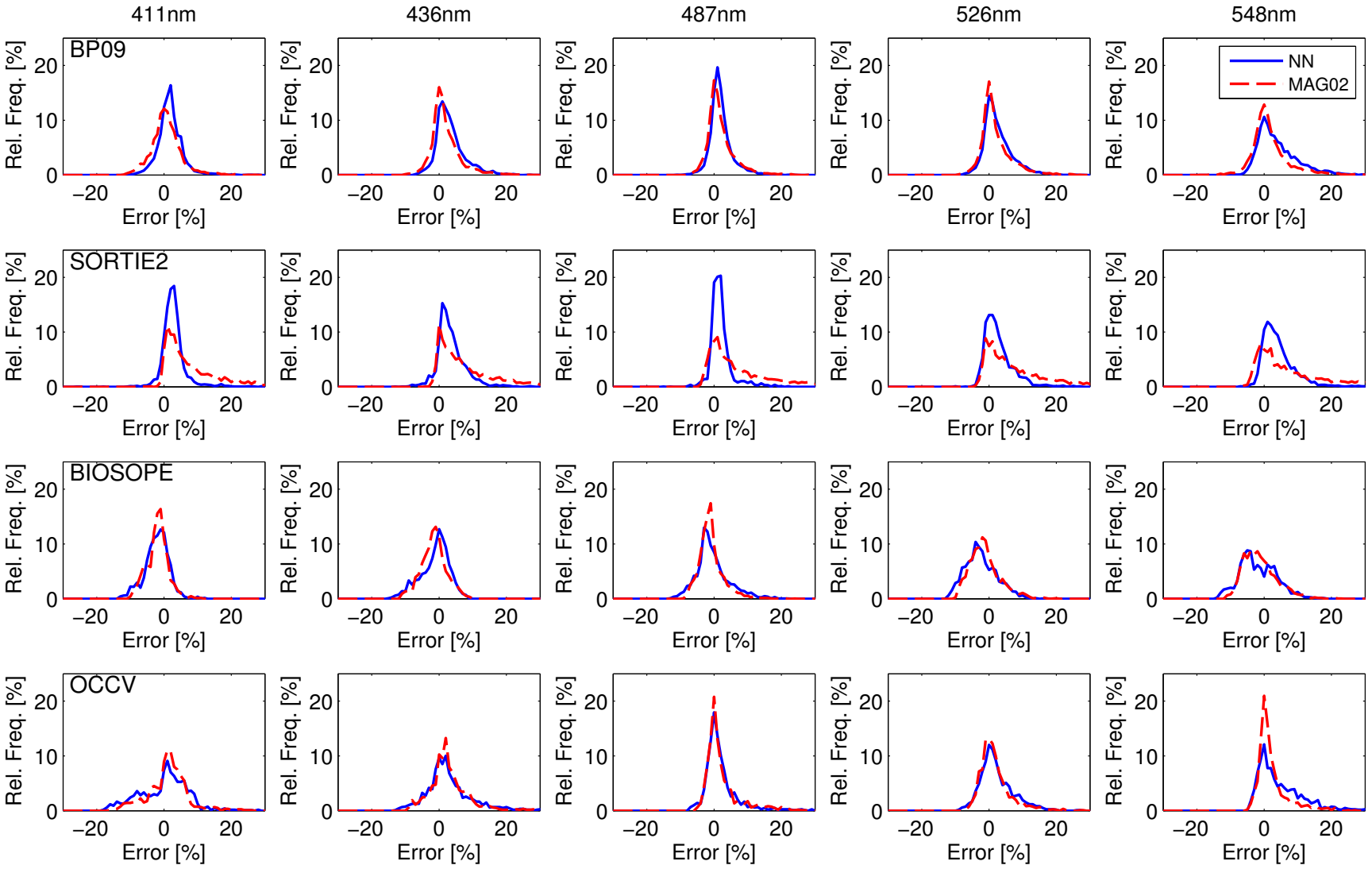

Comparison between MAG02 and RBF-NN method using NuRADS data.

Light and Life Laboratory
STEVENS Institute of Technology

Summary

- A neural network method was developed to correct for bidirectional effects in remote sensing reflectances.
- The method was validated using synthetic data as well as NuRADS field measurements.
- This BRDF correction method does not require any knowledge of the inherent optical properties of the water.
- Its performance is similar to that of the MAG02 method in chlorophyll-dominated (open ocean) water, but significantly better in turbid (coastal) water.
- This BRDF correction method is expected to improve the accuracy of marine parameters in turbid coastal waters inferred from retrieval methods that rely on nadir-converted remote sensing reflectances.

Light and Life Laboratory STEVENS Institute of Technology

NEXT: Sunglint Study

Simulation of glint reflectance and determination of surface roughness of turbid coastal and inland aquatic waters

Zhenyi Lin[a], Yongzhen Fan[a], Wei Li[a], Charles Gatebe[b,c], and Knut Stamnes[a]

[a]Light and Life Laboratory
Department of Physics
Stevens Institute of Technology
Hoboken, New Jersey, USA

[b]NASA Goddard Space Flight Center, Greenbelt, Maryland, USA

[c]Universities Space Research Association, Columbia, Maryland, USA

For details see: Z. Lin, W. Li, C. Gatebe, R. Poudyal, and K. Stamnes, Radiative transfer simulations of the two-dimensional ocean glint reflectance and determination of the sea surface roughness, Applied Optics, 55, 1206-1215, 2016.

Atmosphere correction of glint

SeaDAS algorithm contains corrections of:

- 1-D direct beam reflectance

$$I_{\text{glint}}^{\text{TOA}}(\mu_0, \mu, \Delta\phi) = F_0(\lambda) T_0(\lambda) T(\lambda) I_{\text{GN}}$$

$$T_0(\lambda) T(\lambda) = \exp\left\{ -[\tau_M(\lambda) + \tau_A(\lambda)] \left(\frac{1}{\mu_0} + \frac{1}{\mu} \right) \right\}$$

- diffuse light reflectance (skyglint) (considered in a Rayleigh lookup table)

What is missed?

- diffuse light reflectance from aerosols mixed with molecules in surface layer (forward scattering)
- 2-D feature of sunglint

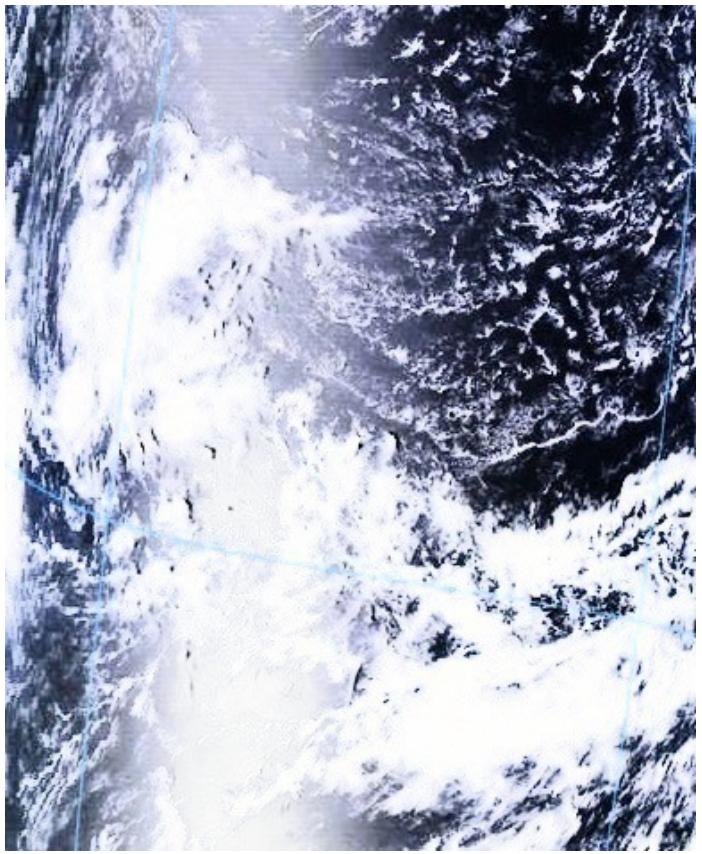

Glint contamination in MODIS image

Radiative transfer forward model

- Accurate computation of diffuse light reflectance (enhanced AccuRT)
- Consistent computation of aerosol and molecular scattering

Radiative Transfer Model

DISORT 3 (implemented in AccuRT)

- 1-D Discrete-Ordinate Radiative Transfer model
- updated version 3 in 2015 – http://lllab.phy.stevens.edu/disort/

Modeling difficulty:

$$\textbf{Phase function: } p(u,u',\Delta\phi) \approx \sum_{m=0}^{M-1}(2-\delta_{0m})p^m(u,u')\cos m(\Delta\phi)$$

$$\textbf{BRDF: } \rho(u,u',\Delta\phi) \approx \sum_{m=0}^{M-1}\rho^m(u,u')\cos m(\Delta\phi)$$

The expansion of the phase function $p(u,u',\Delta\phi)$ and the BRDF is symmetric about the principal plane and intrinsically one-dimensional. Therefore:

- a 1-D BRDF is incapable of simulating the directional dependence of realistically anisotropic surfaces.

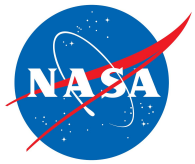

Radiative Transfer Model

Pseudo two-dimensional BRDF

- Use 2-D BRDF to compute the **direct** beam reflectance
- Use 1-D BRDF to compute the **diffuse** light reflectance

$$I_{\text{up,refl}}(\tau_{\text{atm}}, \mu', \phi') = \mu_0 \, \rho_{2-\text{D}}(\mu_0, \mu', \phi') F_0 \, e^{-\tau_{\text{atm}}/\mu_0} + \int_0^{2\pi} \int_0^1 \mu \, \rho_{1-\text{D}}(\mu, \mu', \Delta\phi) I_{\text{down,inc}}(\tau_{\text{atm}}, \mu, \phi) d\mu d\phi$$

Gaussian rough sea surface

The surface slope variance follows a Gaussian distribution:

- **2-D Gaussian surface for direct beam reflectance**
- **1-D Gaussian surface for diffuse light reflectance**

$$p(z_c, z_u) = \frac{1}{2\pi\sigma_c\sigma_u} \exp\left[-\frac{1}{2}\left(\frac{{z_c}^2}{\sigma_c^2} + \frac{{z_u}^2}{\sigma_u^2}\right)\right] \qquad p(\mu_n, \sigma) = \frac{1}{\pi\sigma^2} \exp\left(-\frac{\tan^2\theta_n}{\sigma^2}\right)$$

$$\frac{\sigma^2}{2} = \sigma_c^2 + \sigma_u^2, \qquad u \equiv \text{upwind}, \qquad c \equiv \text{crosswind}$$

We did not parameterize $\sigma_{c,u}$ and σ with wind speed!

BRDF Measurement from airplane

(a) NASA P-3B Aircraft

(b) CAR Schematic

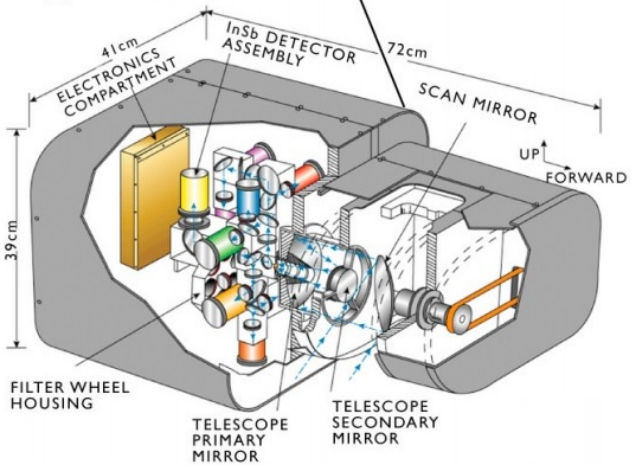

(c) Flight Track during BRDF Measurements

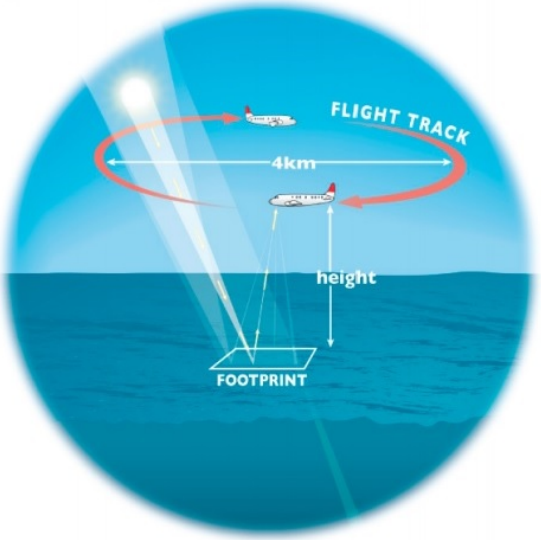

(d) Cloud Absorption Radiometer (CAR) Parameters

Angular Scan Range	190°
Instantaneous field of view	17.5 mrad (1°)
Pixels per scan line	382
Scan rate	1.67 lines per second (100 rpm)
Spectral channels (μm; bandwidth (FWHM)	14 (8 continuously sampled and last six in filter wheel: 0.340(0.009), 0.381(0.006), 0.473(0.021) 0.683(0.021), 0.871(0.022), 1.037(0.021), 1.222(0.023), 1.275(0.023), 1.564(0.032), 1.657(0.042), 1.738(0.040), 2.105(0.045), 2.202(0.043), 2.303(0.044)

The measurements were obtained under clear sky conditions from the NASA Cloud Absorption Radiometer (CAR) deployed aboard the University of Washington Convair 580 (CV-580) research aircraft. The airplane flew in a circle about 3 km in diameter, taking roughly 2-3 minutes to complete an orbit about 200 m above the surface.

Retrieval method

Forward model F(x): DISORT 3 with pseudo 2-D BRDF

Wavelength: 1,036 nm, no water leaving radiance

- Molecular layer: $\varpi_{\text{mol}} = 0.961$, $\tau_{\text{mol}} = 0.00645$
- Aerosols & molecules mixed layer: $\varpi_{\text{mix}} = (\beta_{\text{mol}} + \beta_{\text{aer}})/(\gamma_{\text{mol}} + \gamma_{\text{aer}}) = 0.9772$
- Total optical thickness above airplane: $\tau_{\text{airplane}} = \tau_{\text{mol}} + 0.9\tau_{\text{mix}}$
- Model output: upward radiance at arbitrary angle

Measurements y (bidirectional reflectance factor)

$$\text{BRF}(\mu, \phi, \tau_{\text{airplane}}) = \pi I_{\text{up}}(\mu, \phi, \tau_{\text{airplane}})/\mu_0 F_s$$

with 1° interval in both viewing and azimuth angles.

Gauss-Newton/Levenberg Marquardt non-linear inversion algorithm

$$\mathbf{x} = [\sigma_c^2, \sigma_u^2, \phi_{\text{wind}}, \tau_{\text{mix}}]^T$$

$$\mathbf{x}_{k+1} = \mathbf{x}_k + \left[\mathbf{J}_k^T \mathbf{J}_k + \gamma_k \mathbf{I}\right] \mathbf{J}_k^T (\mathbf{F}(\mathbf{x}_k) - \mathbf{y})$$

Retrieved results

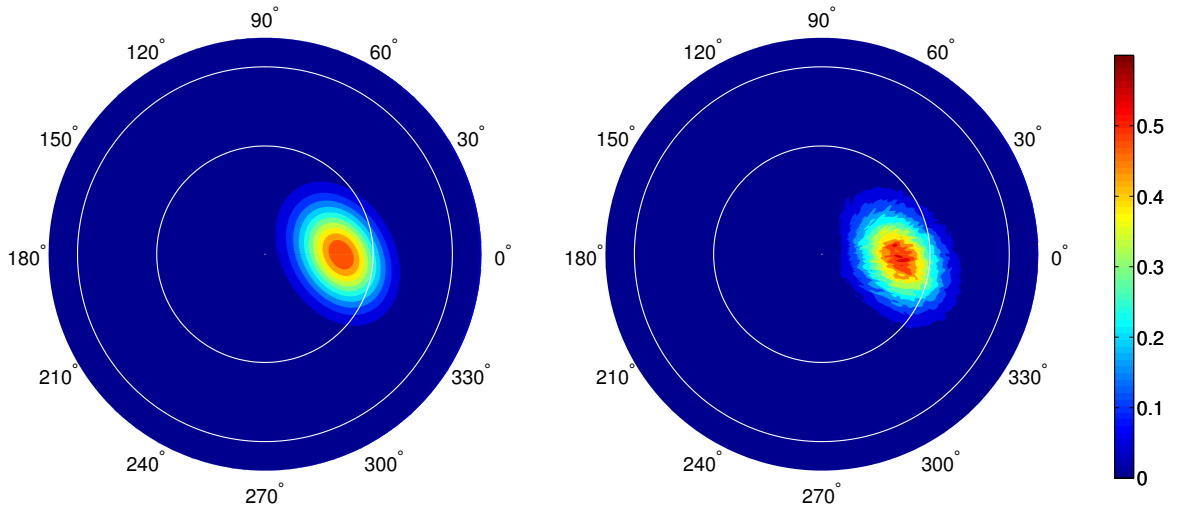

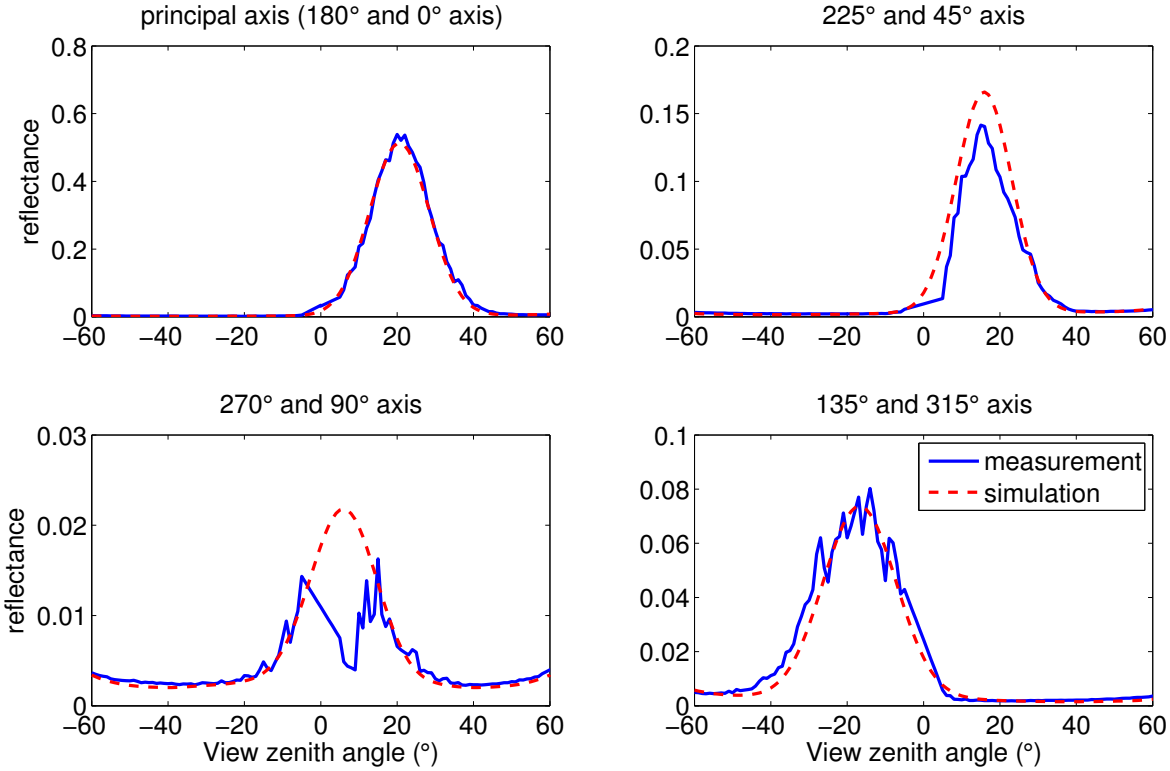

Retrieved results

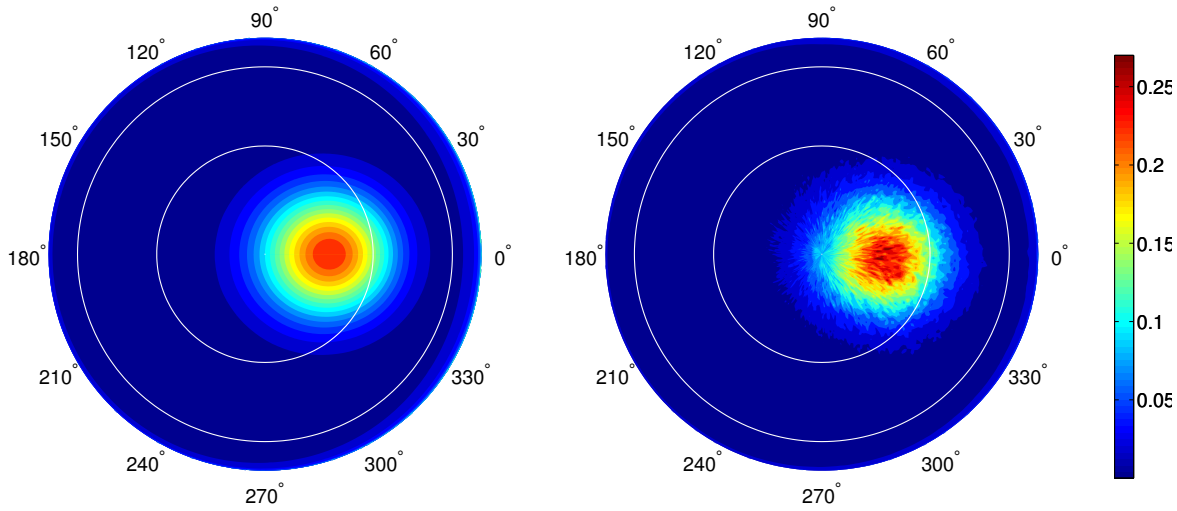

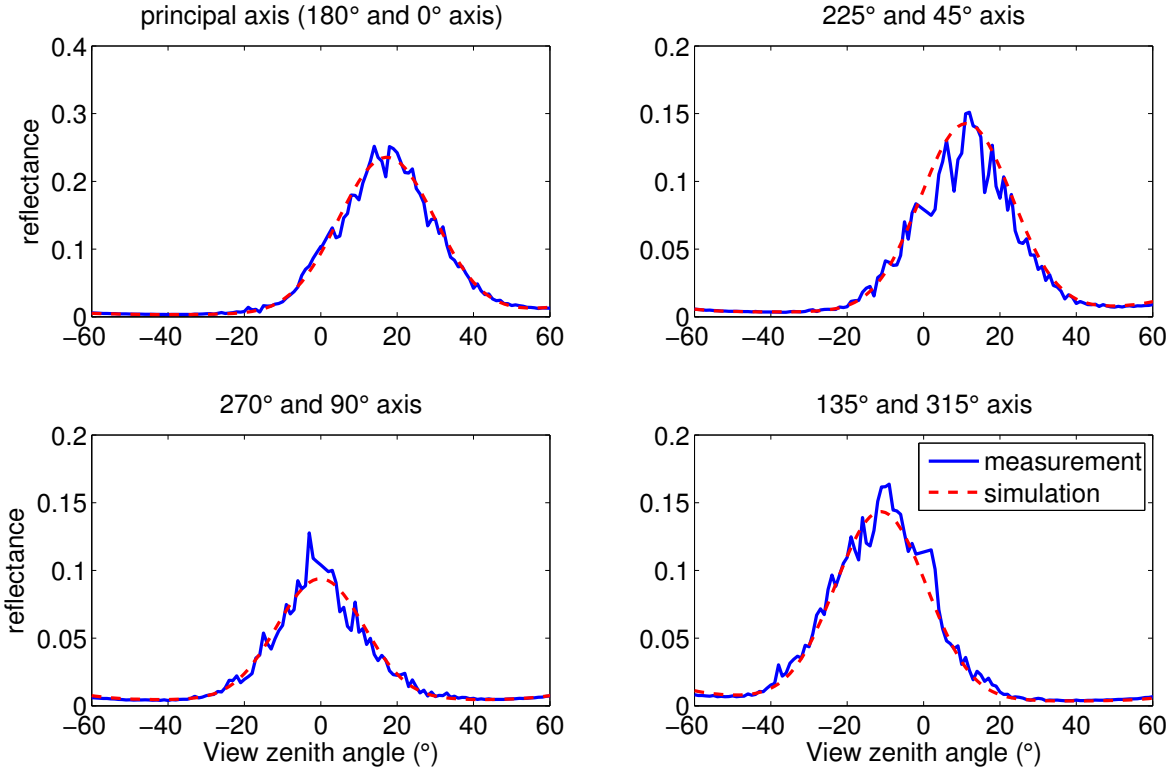

Retrieved results

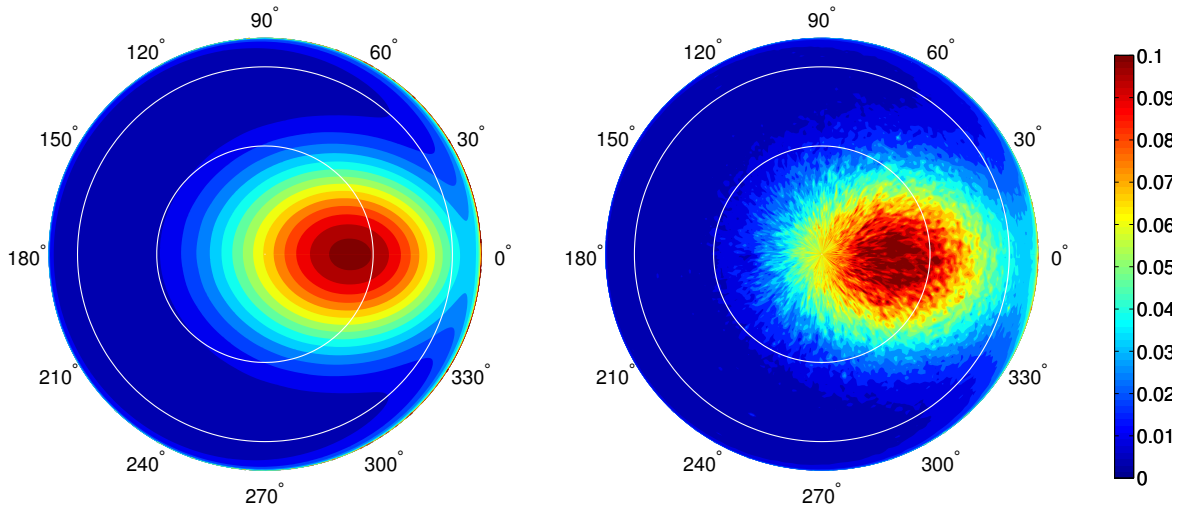

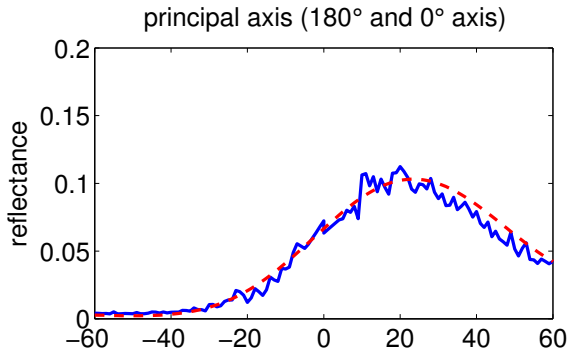

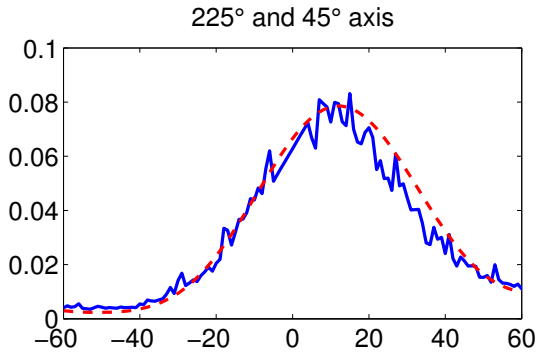

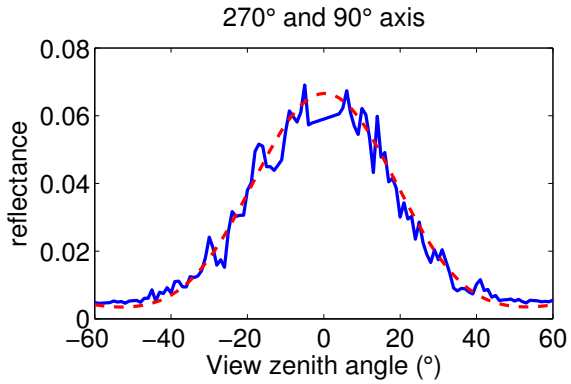

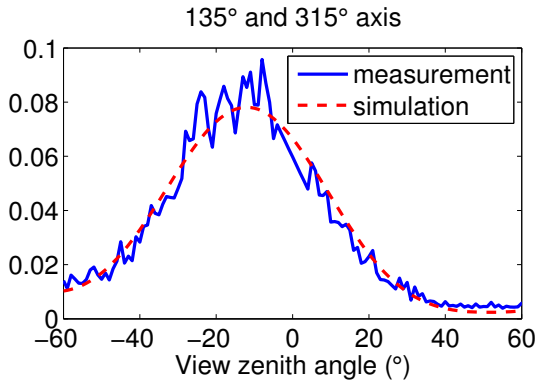

Retrieved results

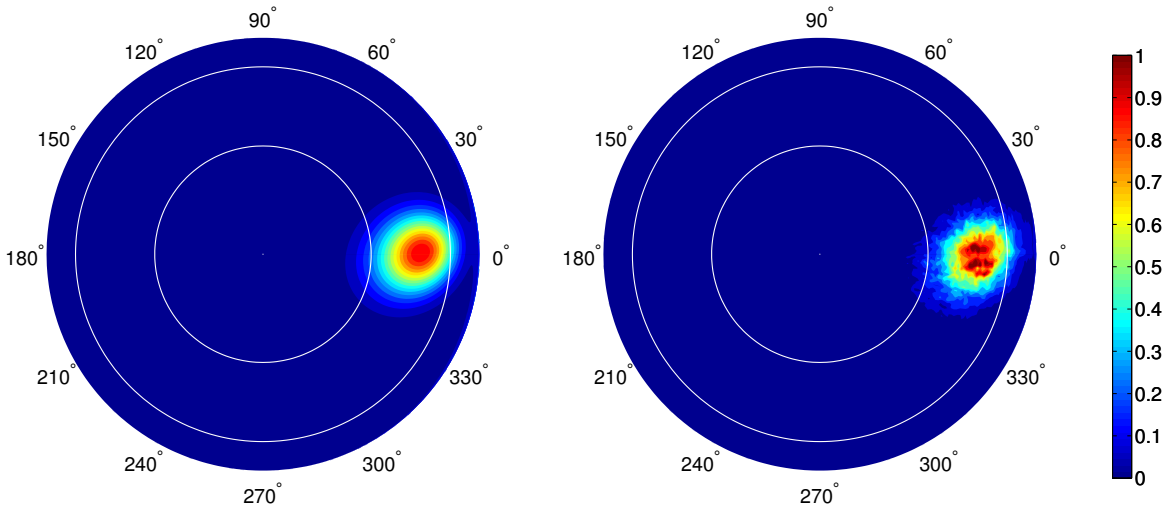

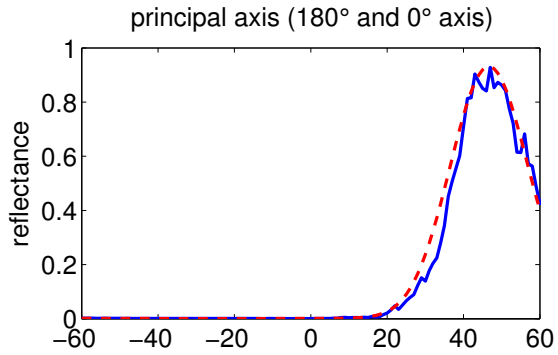

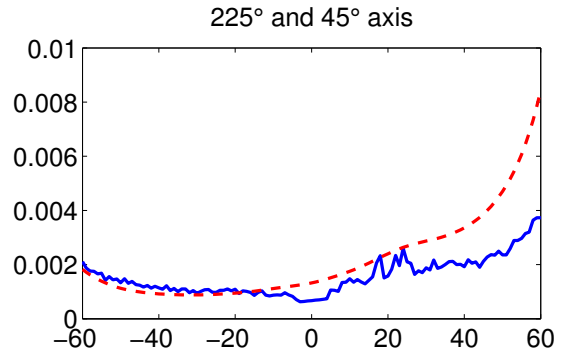

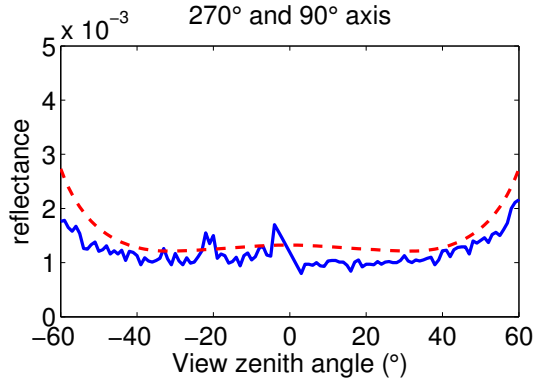

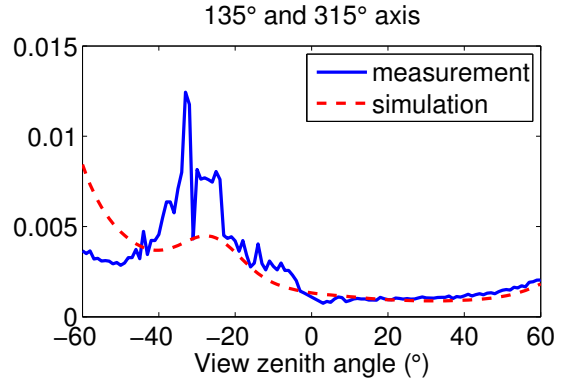

Retrieved results

Retrieved water surface slopes, wind direction (°), and wind speed (m/s)

Date	σ_c^2	σ_u^2	wind speed$_c$ | wind speed$_u$	1-D wind speed	wind direction
10-Jul	0.00747	0.00399	2.29 | 1.23	1.61	31.09
17-Jul	0.01028	0.01162	3.79 | 3.68	3.70	1.92
26-Jul	0.02228	0.03278	10.04 | 10.37	10.17	357.25
02-Aug	0.00802	0.00602	2.61 | 1.90	2.16	313.48

To estimate wind speed, the Cox-Munk glint model is applied:

$$\sigma_c^2 = 0.003 + 0.00192\ \mathrm{W} \pm 0.002$$
$$\sigma_u^2 = 0.000 + 0.00316\ \mathrm{W} \pm 0.004$$
$$\sigma_c^2 + \sigma_u^2 = 0.003 + 0.00512\ \mathrm{W} \pm 0.004$$

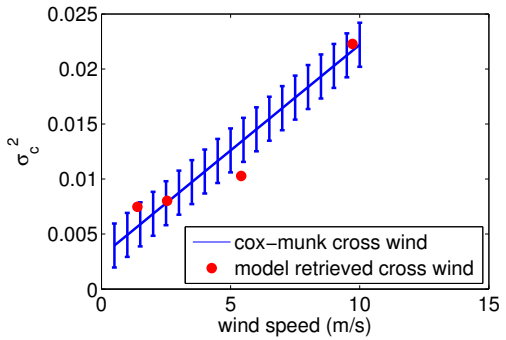

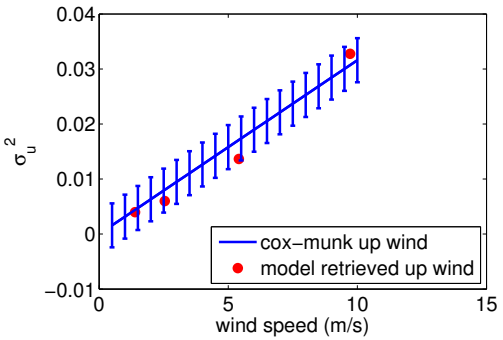

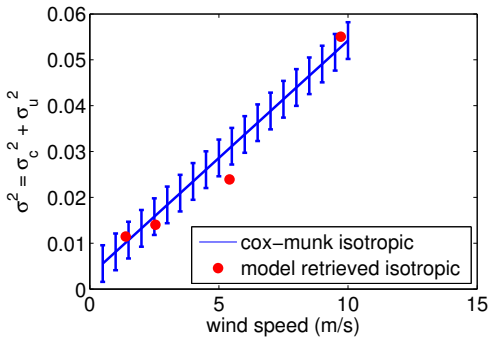

Retrieved results

Retrieved aerosol optical thickness:

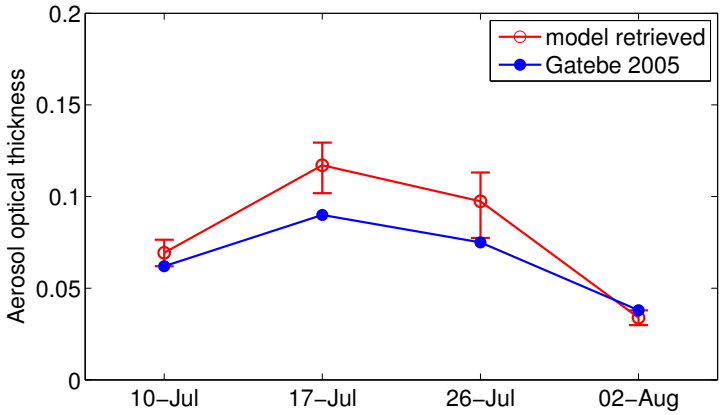

Correlations and histograms for measured and simulated reflectances.

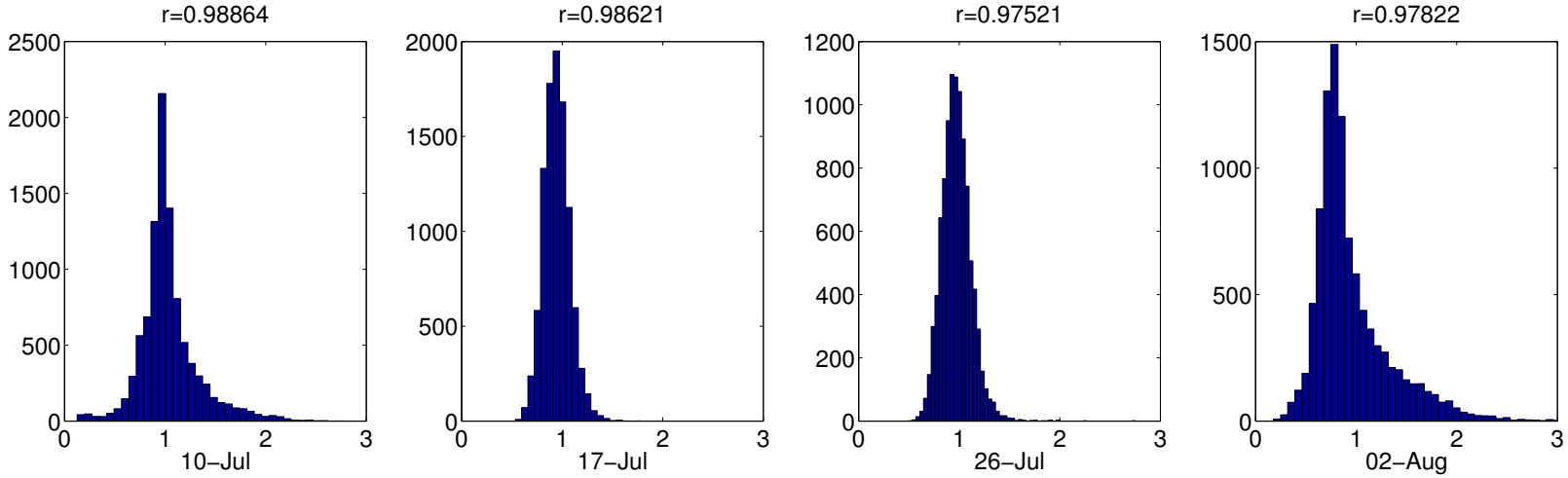

Discussion: 2-D vs 1-D Gaussian surface

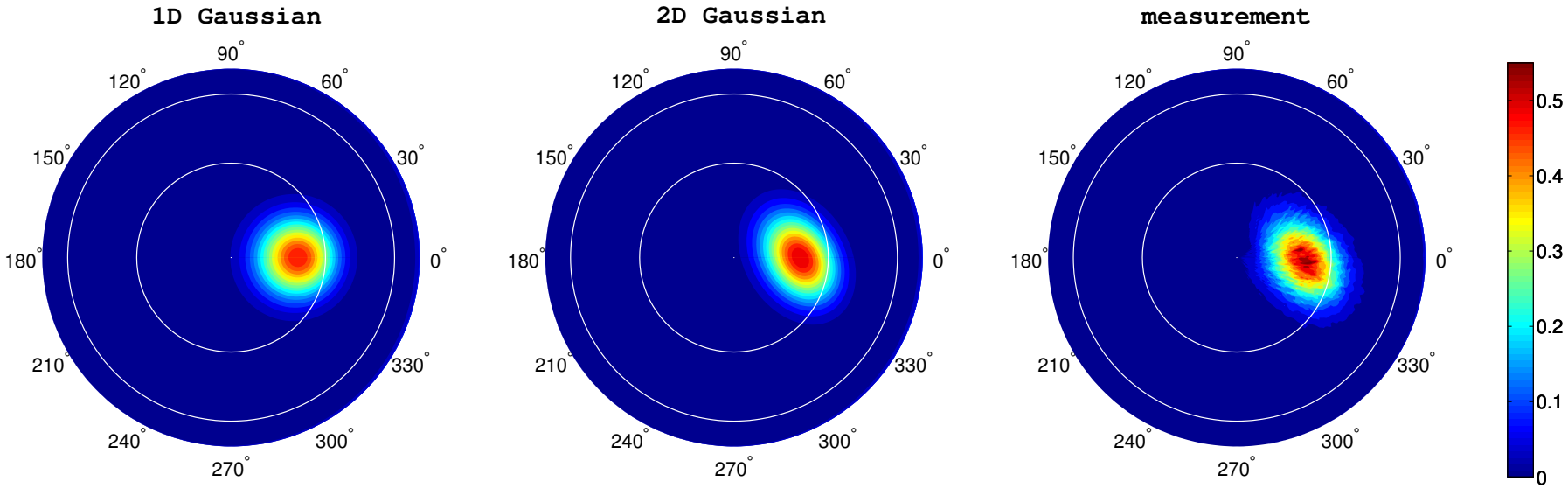

- Model simulations based on a 1-D Gaussian BRDF are unable to match the measured tilted elliptical pattern, but
- a 2-D Gaussian BRDF can reproduce the measurements.

Discussion: reproducing reflectances at 472, 682 and 870 nm

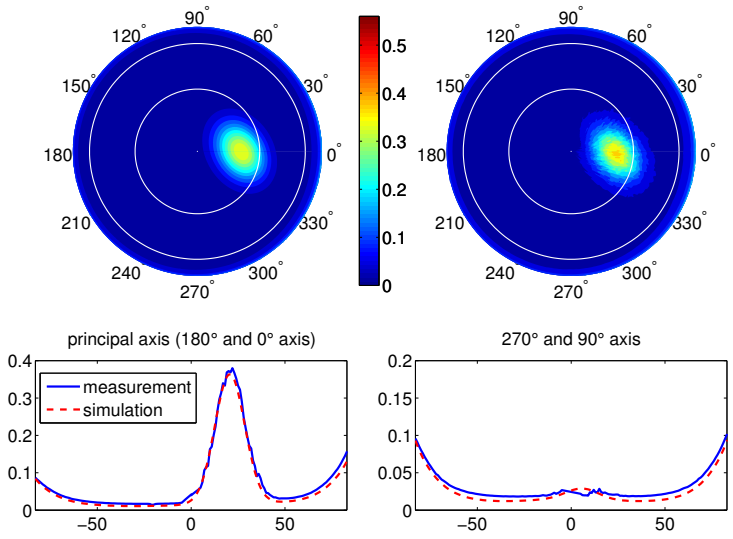

472 nm

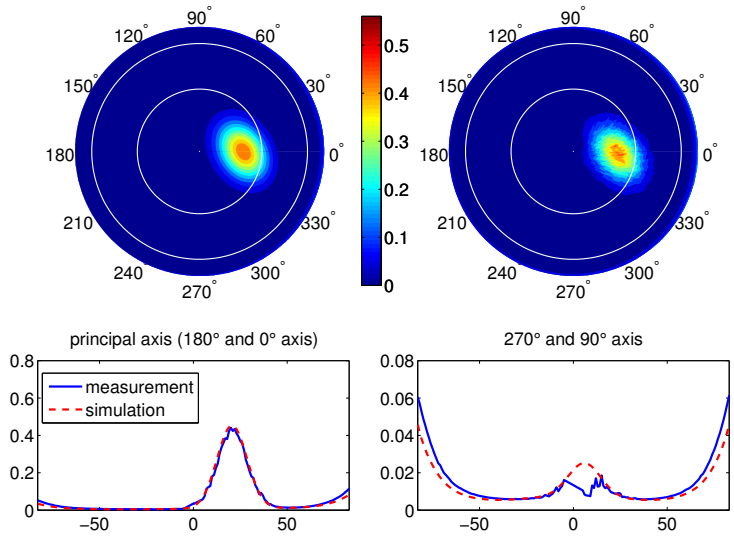

682 nm

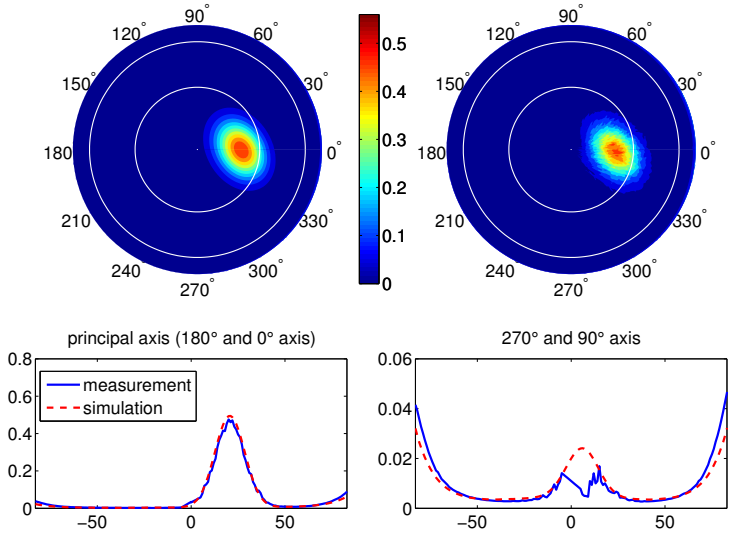

870 nm

We are able to reproduce reflected radiance in the visible bands, with

- surface roughness retrieved from near infrared band at $1,036$ nm
- aerosol and ocean parameters retrieved using visible bands from off-glint geometries.

Summary and Conclusion

- AccuRT was modified to successfully simulate ocean glint.
- NASA CAR data set provides BRDF measurements in 1° intervals for all geometries.
- A pseudo 2-D Gaussian surface BRDF model successfully reproduced the measured tilted elliptical glint pattern (extension: this idea is applicable to any BRDF type).
- The tilted elliptical glint pattern shows the importance of a pseudo 2-D BRDF approach that depends on the wind direction.
- The diffuse light reflectance is also important in the visible channels.

For details see:

Z. Lin, W. Li, C. Gatebe, R. Poudyal, and K. Stamnes, Radiative transfer simulations of the two-dimensional ocean glint reflectance and determination of the sea surface roughness, Applied Optics, 55, 1206-1215, 2016.

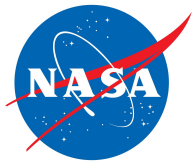

Light and Life Laboratory

STEVENS Institute of Technology

USRA

Next: Remote sensing from geostationary platforms

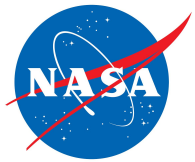

Light and Life Laboratory STEVENS Institute of Technology

USRA

GEO-CAPE Oceans SWG Workshop
NASA Goddard, August 21-22, 2018

Reliable retrieval of atmospheric and aquatic parameters in complex environments based on multilayer neural networks and comprehensive radiative transfer simulations

Yongzhen Fan[a], Wei Li[a], Zhenyi Lin[a], Charles Gatebe[b,c], Jae-Hyun Ahn[d], Wonkook Kim[d], Knut Stamnes[a]

[a] Light and Life Laboratory, Department of Physics, Stevens Institute of Technology, Hoboken, New Jersey, USA
[b] NASA Goddard Space Flight Center, Greenbelt, Maryland, USA
[c] Universities Space Research Association, Columbia, Maryland, USA
[d]Korea Ocean Satellite Center, Korea Institute of Ocean Science and Technology, Busan, Korea
[h]Department of Physics and Technology, University of Bergen, Bergen, Norway

Generic problem: The small ocean signal!

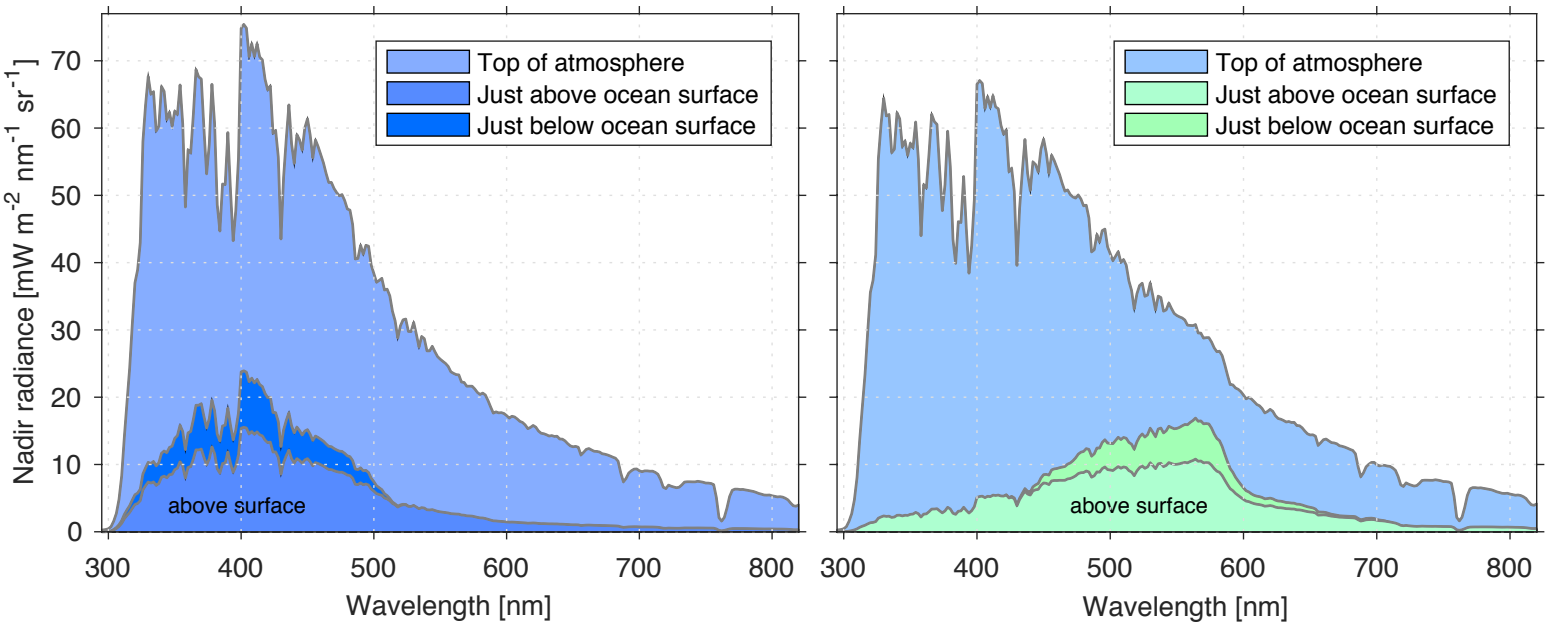

Simulated upward radiance in the nadir direction at (i) the top of the atmosphere, (ii) just **below** the air-water interface, and (iii) just **above** the air-water interface.

Left: Clear **(blue)** water with chlorophyll concentration **0.1** mg m^{-3}.
Right: Turbid **(green)** water with chlorophyll concentration **10** mg m^{-3}.

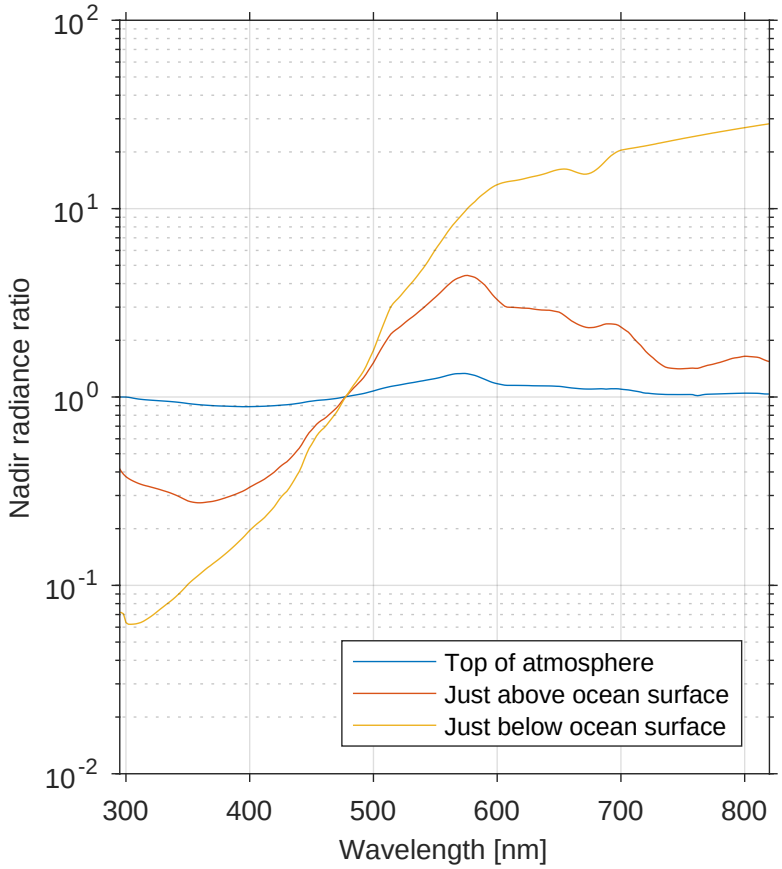

Ratio of simulated nadir radiance for **turbid water** and **clear water** at (i) the top of the atmosphere, (ii) just **below** the air-water interface, and (iii) just **above** the air-water interface.

Frequency of negative Rrs from SeaDAS standard AC

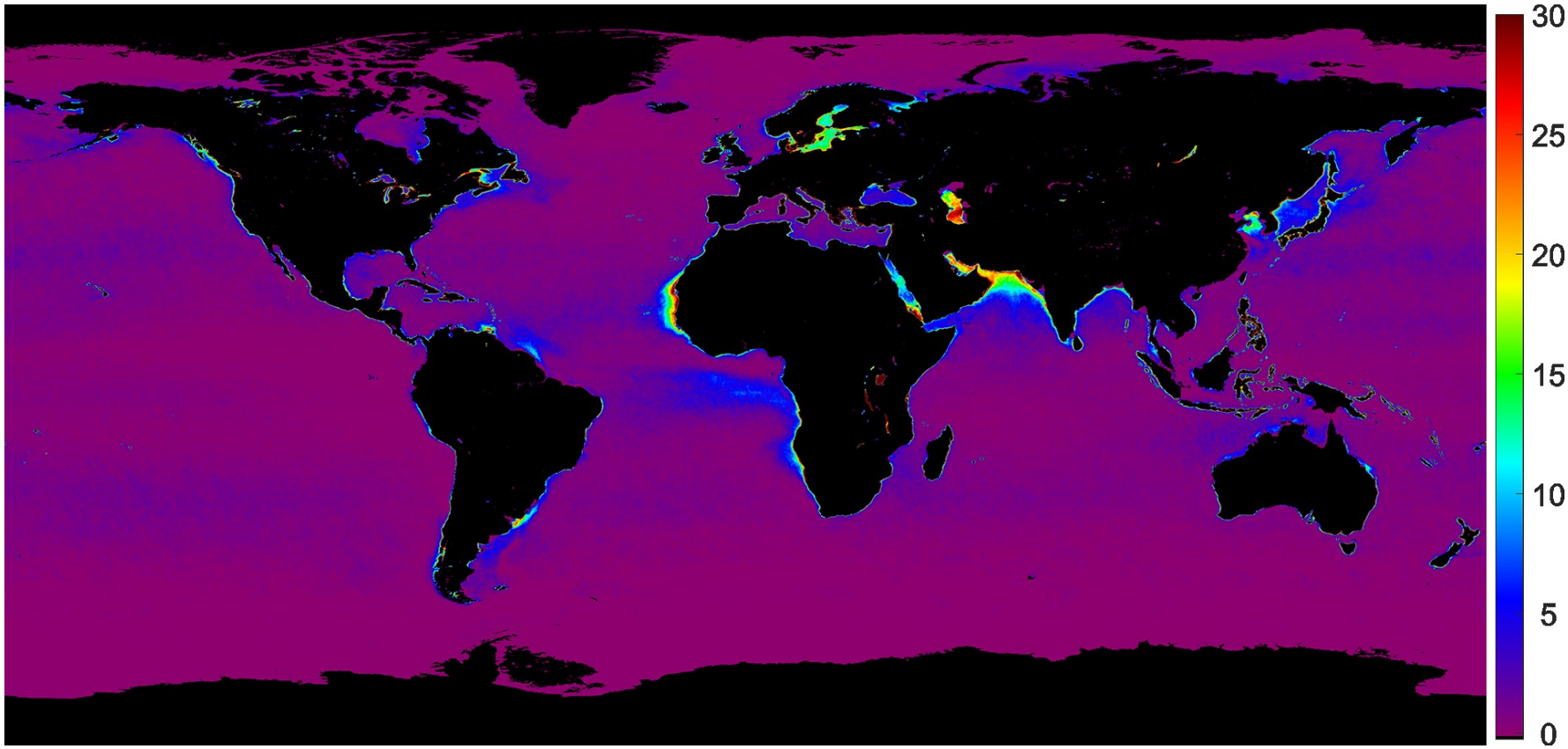

Percentage of negative remote sensing reflectance (Rrs) in 8 day averaged 4 km Aqua MODIS L3 data from 2003-2016

Standard Atmospheric Correction (AC) method

Standard AC algorithms describe the radiance measured by the satellite sensor as:

$$L_t(\lambda) = L_r(\lambda) + L_a(\lambda) + T(\lambda)L_g(\lambda) + t(\lambda)L_{wc}(\lambda) + t(\lambda)L_w(\lambda)$$

L_t	total TOA radiance measured by satellite sensor.
L_r	radiance due to Rayleigh scattering.
L_a	radiance due to aerosols, including Rayleigh-aerosol interaction.
L_g	radiance due to sun glint.
L_{wc}	radiance due to whitecaps.
L_w	water-leaving radiance.
T	direct atmospheric transmittance.
t	diffuse atmospheric transmittance.

The purpose of an AC algorithm is to derive L_w from L_t by removing all the other terms in the equation.

Issues with the standard AC algorithms

- Single scattering approximation
  Solution: use coupled atmosphere-ocean radiative transfer model in simulations, such as **AccuRT**.

- NIR black ocean assumption fails in coastal water (inaccurate aerosol radiances)
  Solution: NIR water-leaving radiance correction
  SWIR – NIR algorithm
  Machine learning algorithm

Multilayer Neural Network (MLNN) Atmospheric Correction method

The most difficult task in standard AC algorithms is to accurately estimate and remove aerosol contribution to TOA radiance.

- **Is it possible to retrieve water-leaving radiance without estimating aerosol radiances?**
  Yes, it is! The spectral similarity between Rayleigh corrected radiance (Lrc) and water-leaving radiance (Lw) implies that AC can be accomplished by properly relating the two spectra.

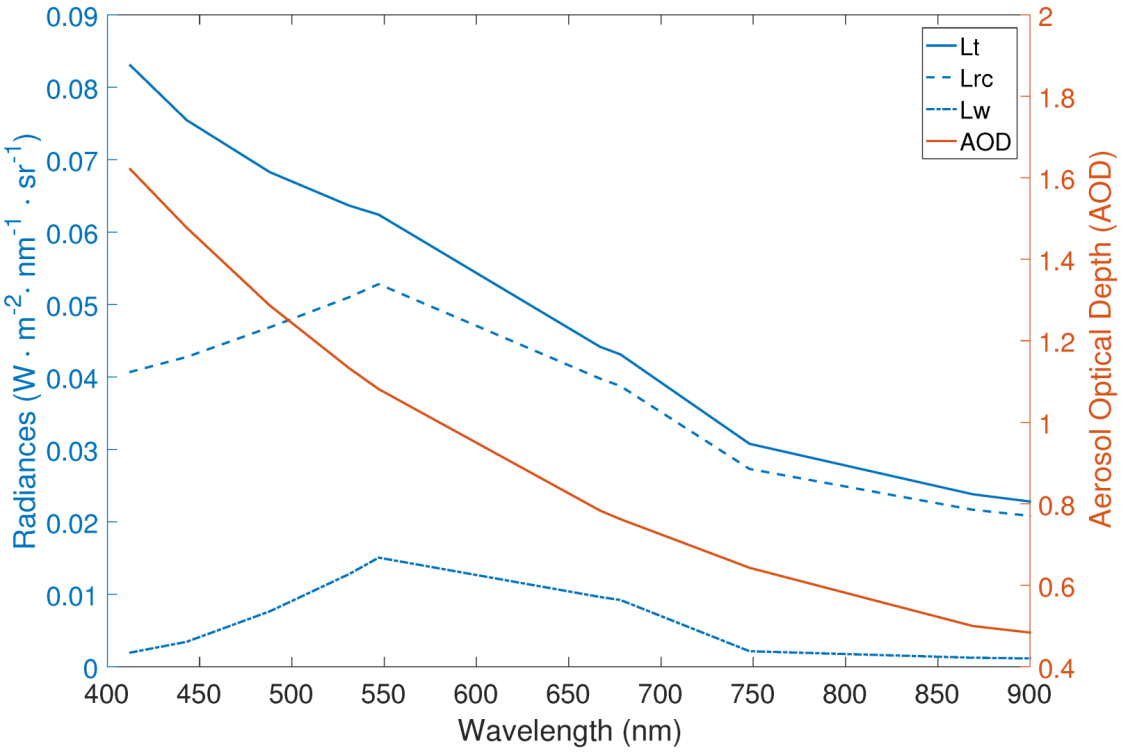

MLNN – Neural network structure

Two retrieval MLNNs were designed and trained:
One for **remote sensing reflectance** (Rrs = Lw/Ed^{0+}) and another **one for AOD**.

Rrs MLNN (50X20X15)

Input: SZA, VZA, VAA, Lrc at multiple bands (9 for MODIS: 412, 443, 488, 531, 547, 667, 678, 748, 869 nm)
Output: normalized Rrs at visible bands.

AOD MLNN (50X20X15)

Input: SZA, VZA, VAA, Lrc at multiple bands (9 for MODIS 412, 443, 488, 531, 547, 667, 678, 748, 869 nm), RH
Output: AODs at the same bands as input.

Why build separate MLNNs for Rrs and AOD?

- Each MLNN is trained to learn only one type of spectral shape: therefore easier to train and more accurate.
- Errors in one MLNN may not necessarily affect the performance of the other MLNN.

MLNN – Radiative transfer simulation

We used a well-tested **coupled atmosphere-ocean radiative transfer model, AccuRT**, to create synthetic datasets for neural network training and testing purposes.

- For the **clear atmosphere**, we used a **14-layer U.S. standard atmosphere profile**.
- For **aerosols**, we used the **set of aerosol models proposed by Ahmad et al. (2010)**, which is also implemented in the NASA SeaDAS data processing package.
- For the **ocean**, we implemented a **flexible ocean IOP model parametrized in terms of aph(443), adg(443) and bbp(443).** The spectral dependences of the 3 parameters are:
  - $aph(\lambda) = aph(443) \times aph^{*}(\lambda)$, where $aph^{*}(\lambda)$ is the normalized chlorophyll absorption spectrum.
  - $adg(\lambda) = adg(443) \times \exp[-S(\lambda - 443)]$, combined absorption by detrital and dissolved matter
  - $bbp(\lambda) = bbp(443) \times (\lambda/443)^{-\eta}$

Normalized chlorophyll absorption spectra from IOCCG report # 5 and NOMAD database:

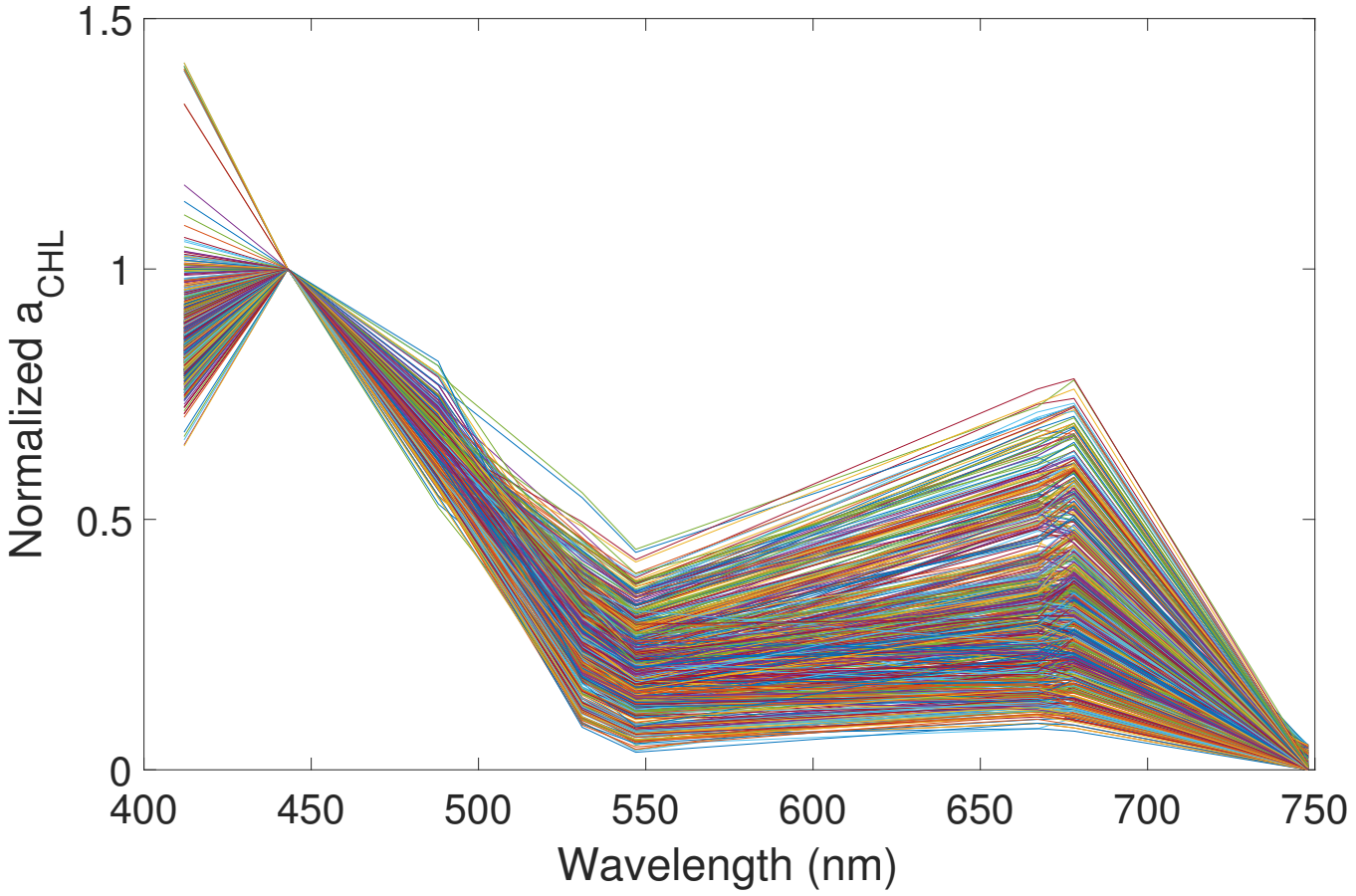

MLNN – Training data generation

Training data should be representative of typical coastal waters. **5 coastal areas (red boxes)** were selected and 8-day 4 km L3 data from 2011-2016 were analyzed to create the input dataset for the RT simulations.

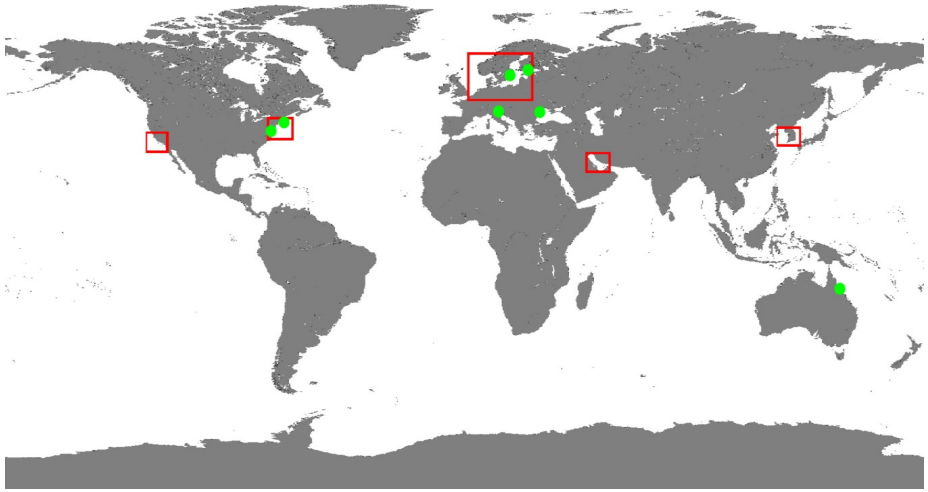

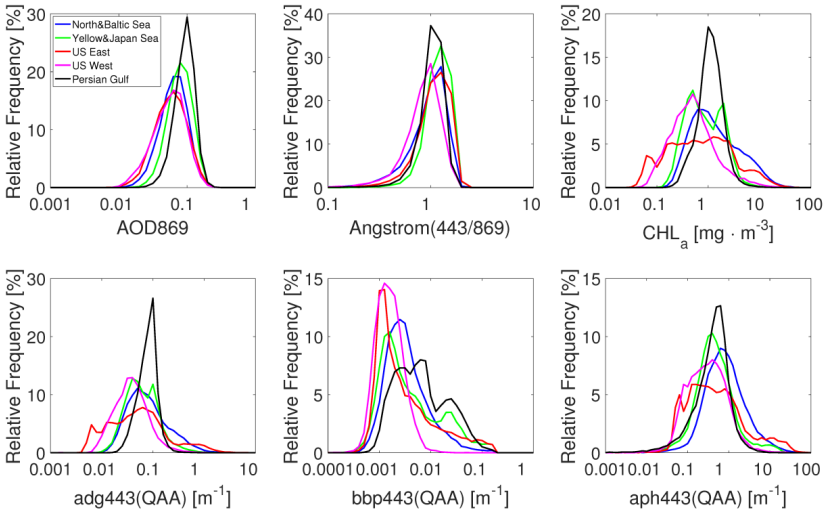

- SZA: 0°-70° random
- VZA: 0°-70° random
- VAA: 0°-180° random

- AOD(869): 0.005-0.35 from L3
- Fraction: 0-1 random
- RH: 20%-99% random

- aph(443): 0.001-95 [m^{-1}] from L3
- adg(443): 0.001-8 [m^{-1}] from L3
- bbp(443): 0.00002-0.2 [m^{-1}] from L3
- aph: random selection from 299 spectral measurements
- adg S: 0.008-0.026 random
- bbp_η: Gaussian random μ=1.0, σ=0.2

MLNN – Validation based on AERONET-OC data

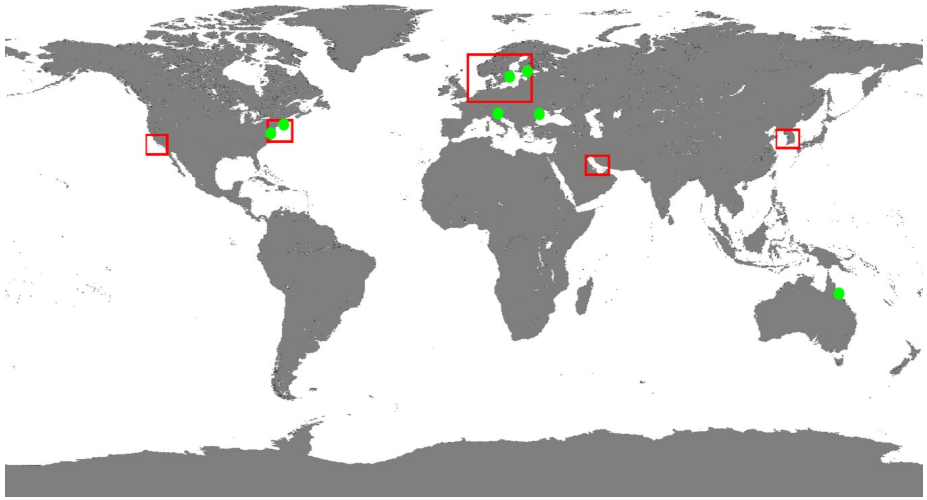

AERONET-OC v2.0 data (N=20,813) from **7 stations** (green dots) **: AAOT, COVE, MVCO, HLT, GDLT, GLORIA, LUCINDA**

Time: 2002- 2015

Algorithms:
SeaDAS NIR, SeaDAS NIR/SWIR, MLNN and C2RCC

MODIS collection 6 L1B data processed by NASA SeaDAS v7.3.2 and ESA SNAP software.

MODIS and AERONET-OC data Matchup

- Time difference < ± 1 hour, for redundant data, only the one with minimum time difference was accepted.
- MOIDS data from a 3X3 box (nine pixels) centered at the AERONET-OC station were processed. Pixels flagged by SeaDAS (i.e. cloud, glint, high solar or sensor zenith angles, etc.) were excluded.
- Pixels marked as out of scope by AANN (auto-associative neural network) were excluded.
- Boxes with less than six pixels available after screening were excluded.
- Boxes with significant spatial heterogeneity were excluded (CV > 0.2). CV=standard deviation / mean value.

Data points available after matchup: N = 1709

MLNN – Validation on AERONET-OC data (AOD)

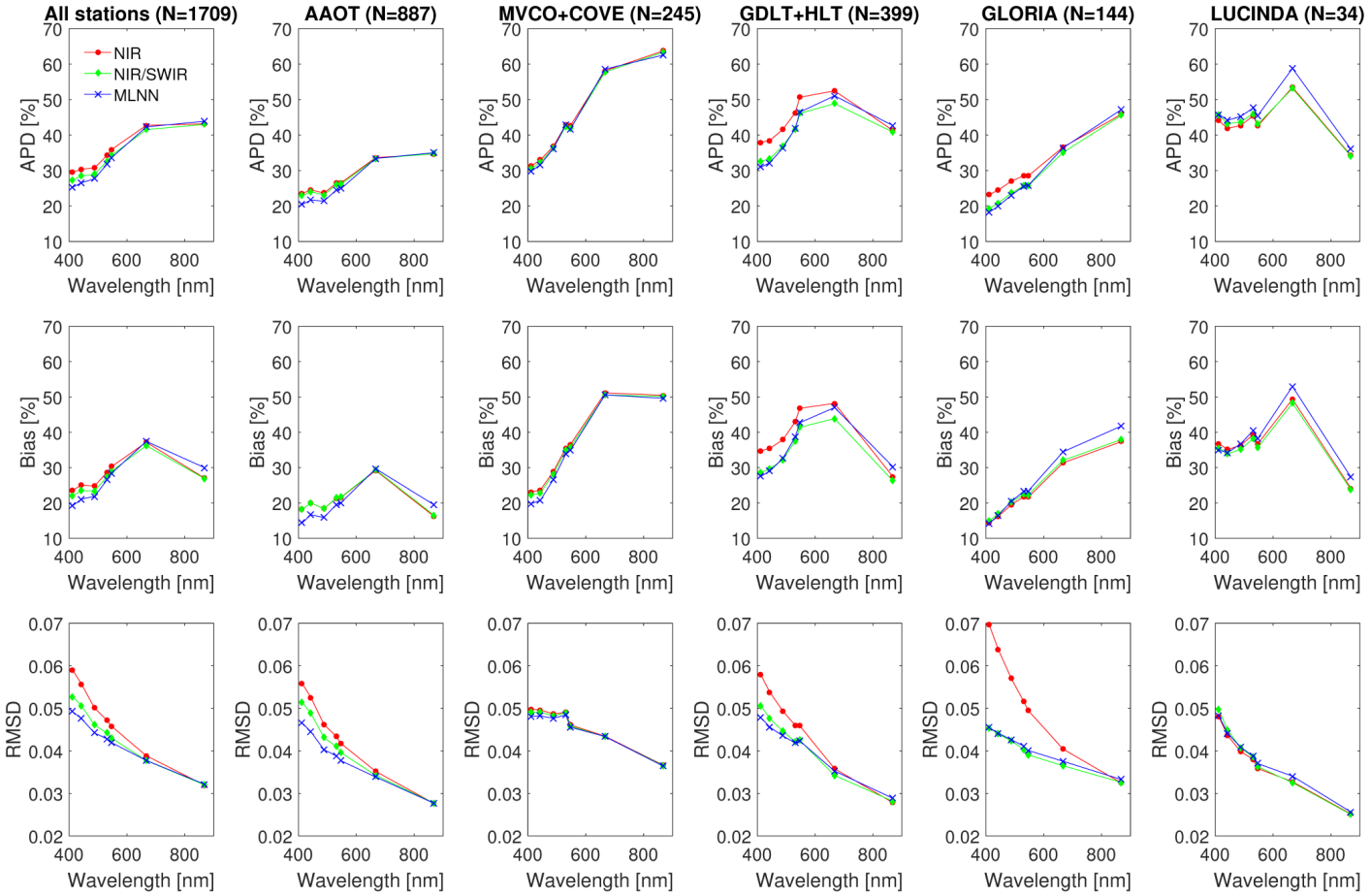

MLNN – Validation on AERONET-OC data (nLw)

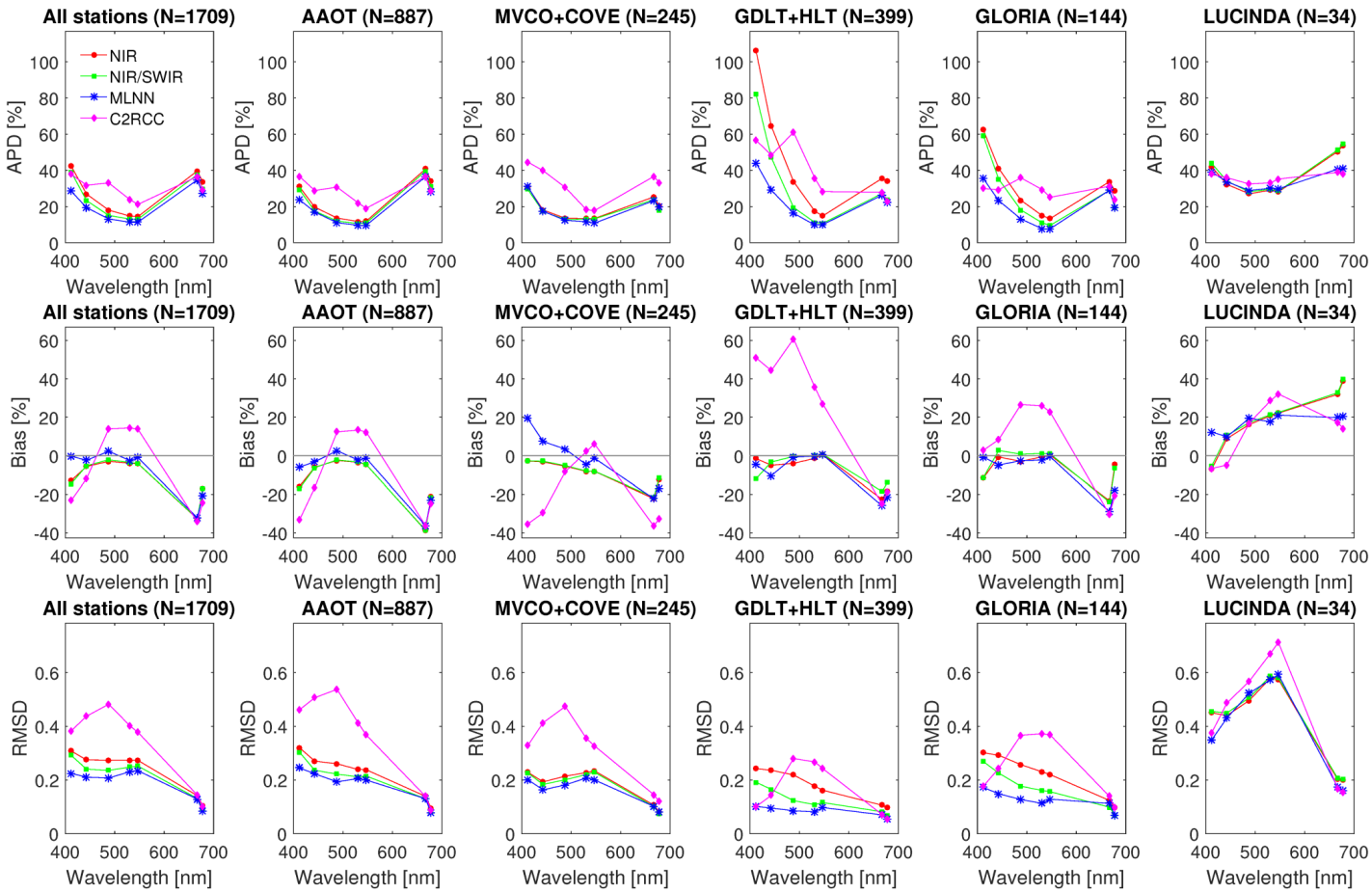

MLNN – MODIS image comparison

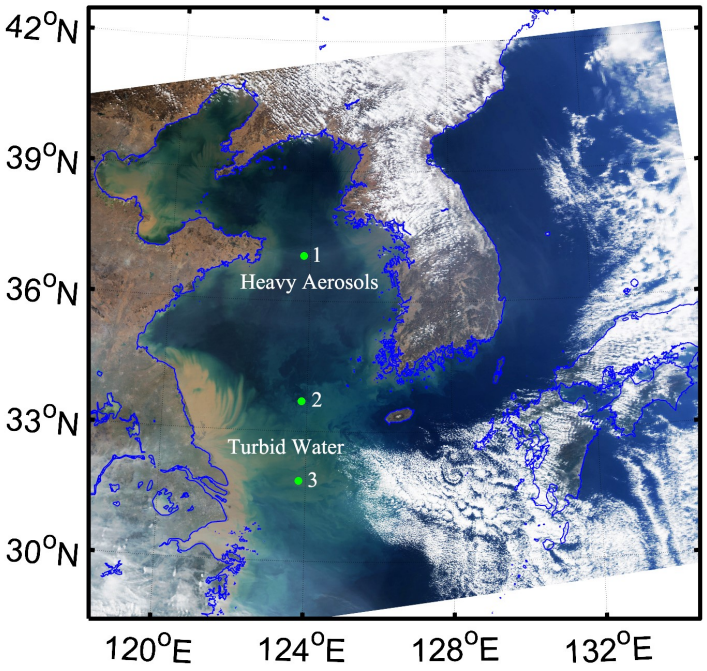

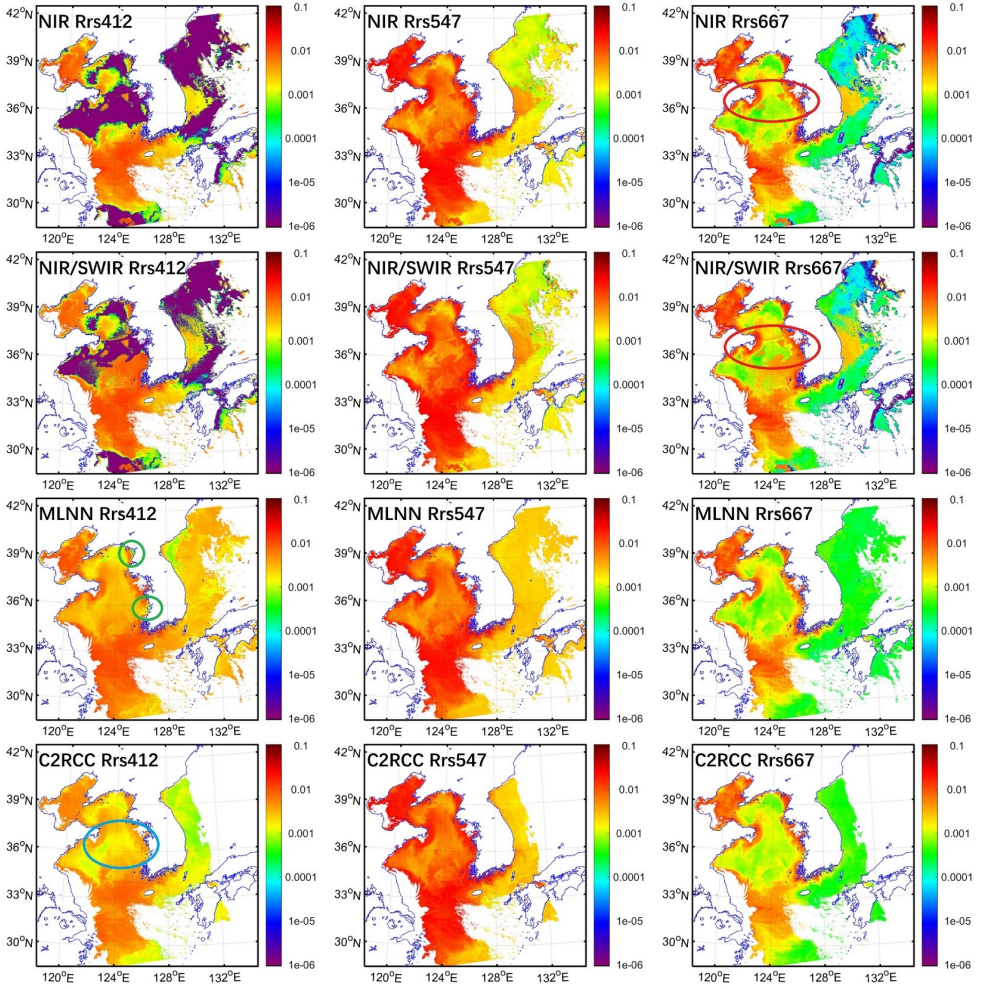

MLNN – MODIS image comparison

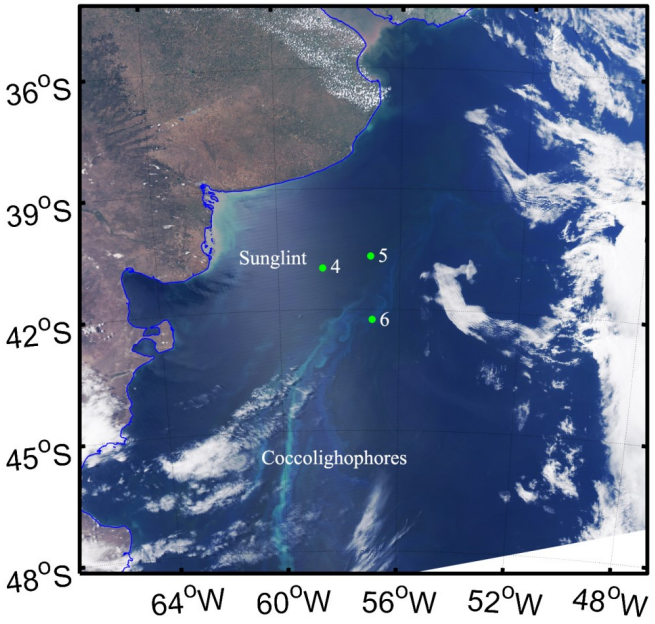

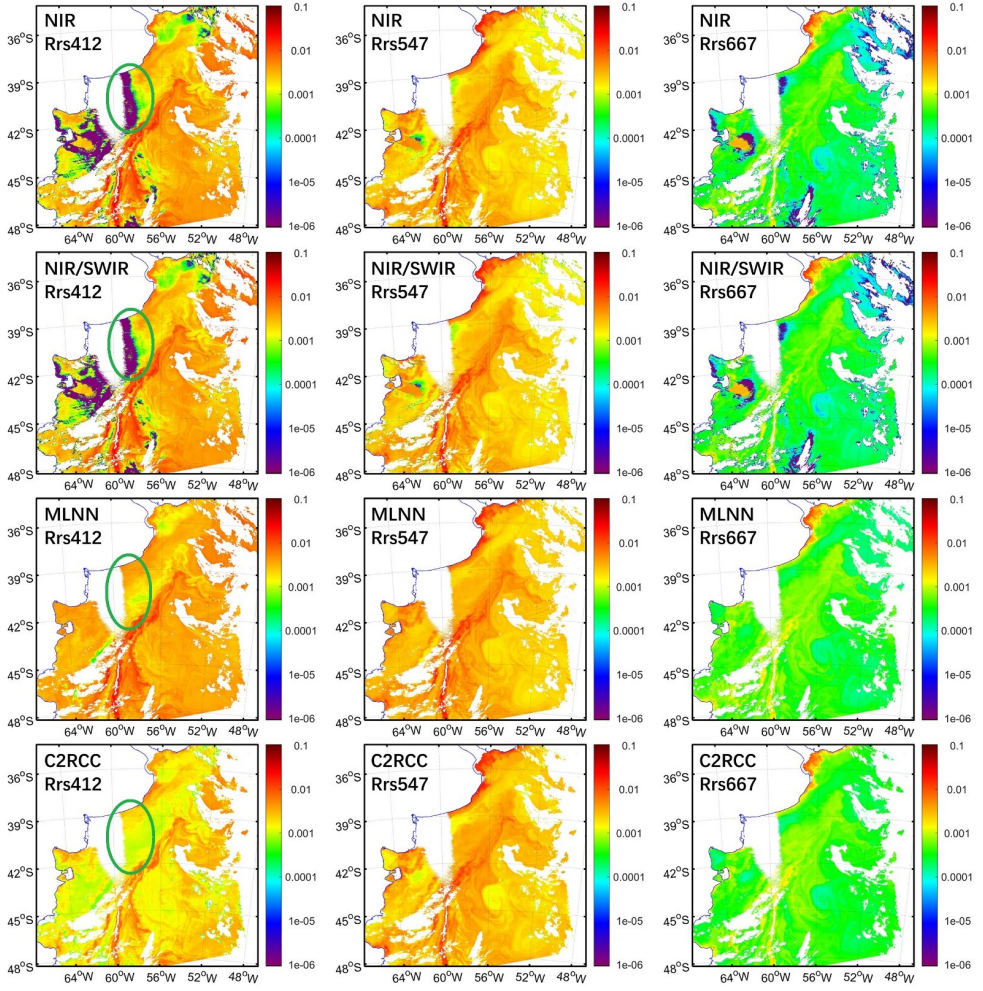

Beyond normal conditions (polluted continental aerosol and extremely turbid water)

- The MLNN algorithm is applicable to heavily polluted continental aerosols and extremely turbid water conditions.

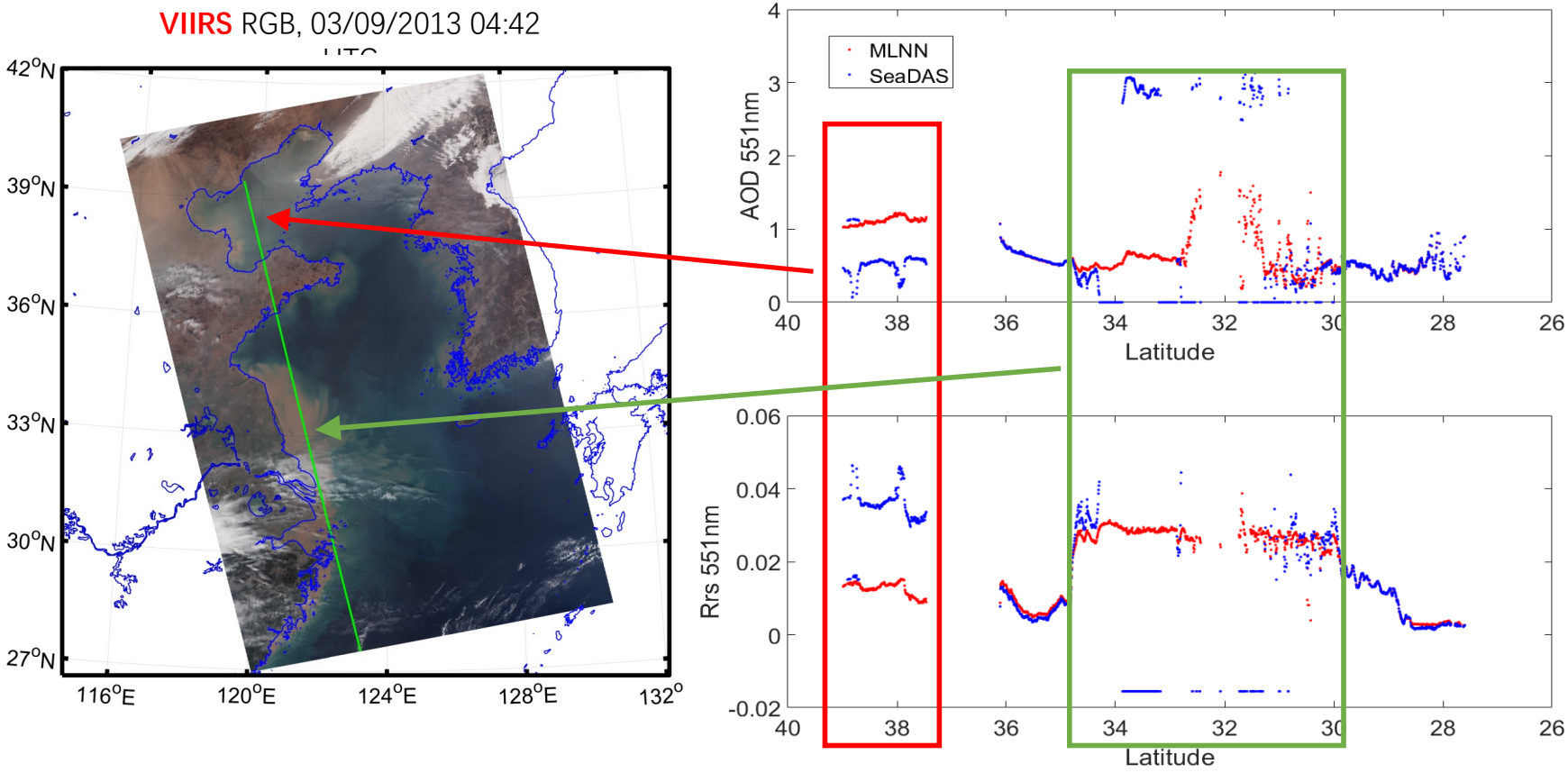

Beyond normal conditions (polluted continental aerosol and extremely turbid water)

- MLNN algorithm significantly improves Rrs retrieval in areas with heavily polluted aerosols and turbid water. The standard SeaDAS algorithm produces a large number of **negative Rrs (purple color)** and **large areas with no retrievals**.

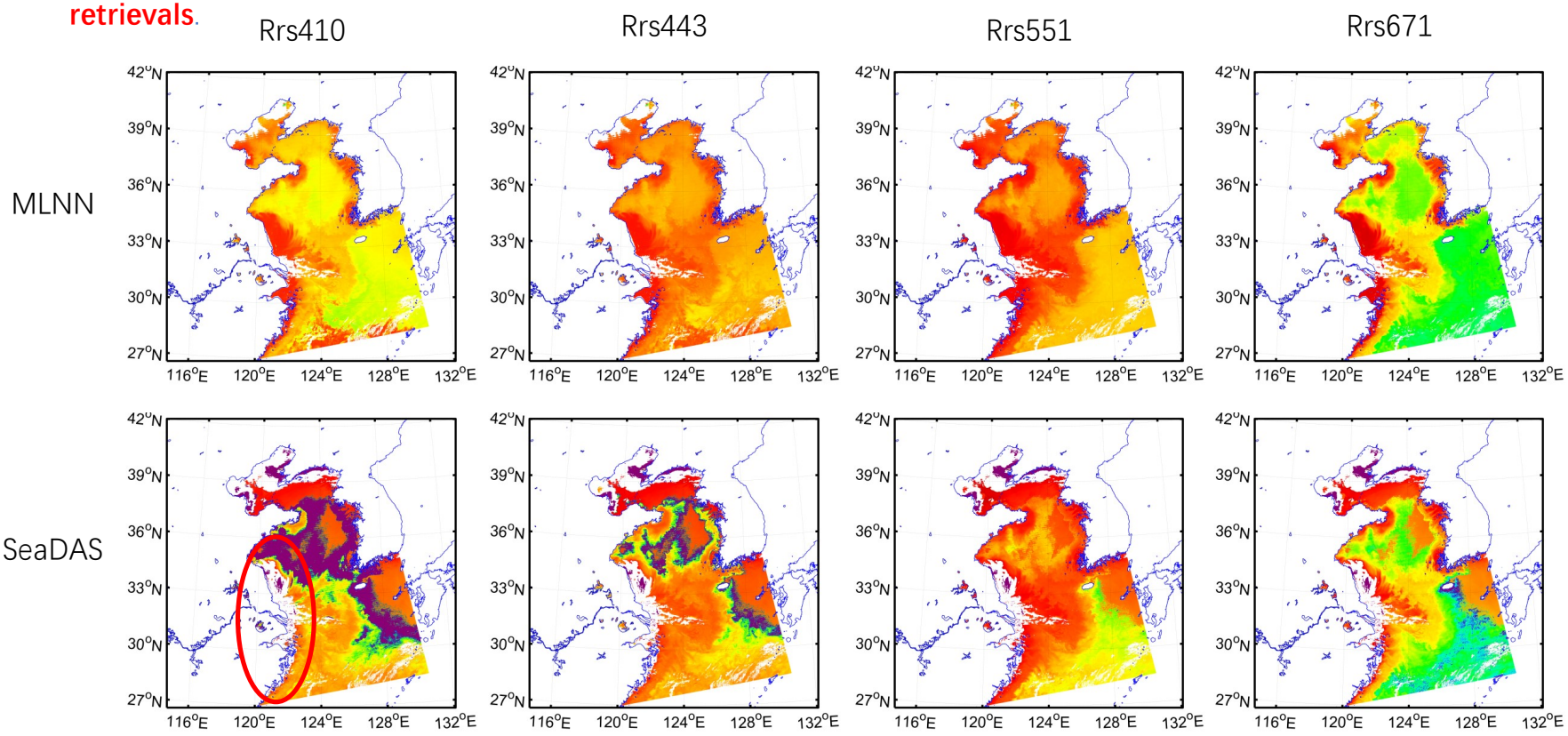

Beyond normal conditions (polluted continental aerosol and extremely turbid water)

- In areas with heavily polluted aerosols and extremely turbid water, the **MLNN algorithm improves AOD retrieval**, whereas the standard **SeaDAS algorithm produces unreasonable** and **abrupt transitions**.

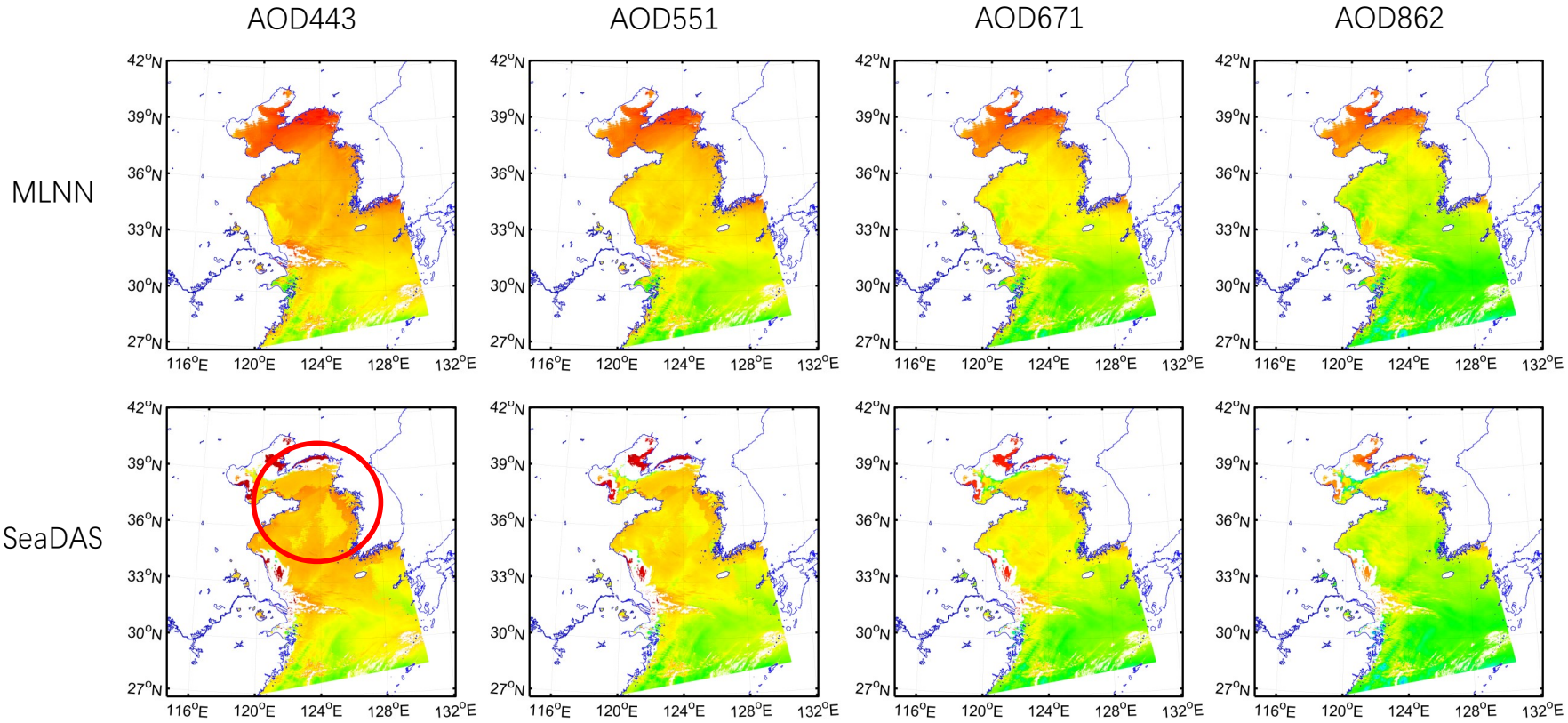

GEO-CAPE Oceans SWG Workshop
NASA Goddard, August 21-22, 2018

Summary

- The Multilayer Neural Network (MLNN) algorithm **improved the quality of retrieved R_{rs} values**. Overall, the MLNN algorithm reduced average percentage difference (APD) between MODIS retrieval and AERONET-OC data by up to 13% in blue bands and 2%-7% in green and red bands compared to the SeaDAS NIR algorithm.
- In **highly absorbing coastal waters** (Baltic Sea) the MLNN algorithm reduced APD by more than 60%, and in **highly scattering waters** (Black Sea) it reduced APD by more than 25%.
- Image comparisons show that the **MLNN algorithm is robust and resilient to contamination due to sunglint and adjacency effects of land and cloud edges**.
- The MLNN algorithm implicitly **accounts for BRDF effects** and **is applicable in extreme conditions such as heavily polluted continental aerosols, extreme turbid waters, and dust storms.**
- The MLNN algorithm **does not require SWIR bands**, and is therefore suitable for all ocean color sensors.
- **The MLNN algorithm is very fast and suitable for operational use.**
- MLNN algorithm produces a seamless transition between turbid coastal water and clean open ocean water.

Reference

Y. Fan, W. Li, C. K. Gatebe, C. Jamet, G. Zibordi, T. Schroeder and K. Stamnes, Atmospheric correction over coastal waters using multilayer neural networks, Remote Sensing of Environment, **199**, 218-240, (2017).

Geostationary specific issues:
1. Low solar elevations

The **plane parallel approximation (PPA)** breaks down for solar zenith angles larger than about 75°. How do we proceed?

- One option: use the **pseudo-spherical approximation (PSA)** [Eq. (2)]:
  - the direct beam single scattering (solar pseudo-source) term is treated in spherical geometry: $e^{-\tau/\mu_0} \rightarrow e^{-\tau\, Ch(r,\mu_0)} \leftarrow$ **PSA**
  - while the multiple scattering term is treated using the PPA:

$$\mu \frac{dL(\tau,\mu,\phi)}{d\tau} = L(\tau,\mu,\phi) - \overbrace{\frac{\varpi(\tau)}{4\pi}\int_0^{2\pi} d\phi' \int_{-1}^{1} d\mu' p(\tau,\mu',\phi';\mu,\phi) L(\tau,\mu',\phi')}^{\text{multiple scattering}} - \overbrace{\frac{\varpi(\tau)}{4\pi} p(\tau,-\mu_0,\phi_0;\mu,\phi) F_0\, e^{-\tau\, Ch(\mu_0)}}^{\text{single scattering}}. \quad (2)$$

2. Advantage of using a 2-D Gaussian distribution of surface slopes

What about the air-water interface: 1-D or 2-D Gaussian?
Explore advantage of using a 2-D Gaussian distribution of surface slopes?

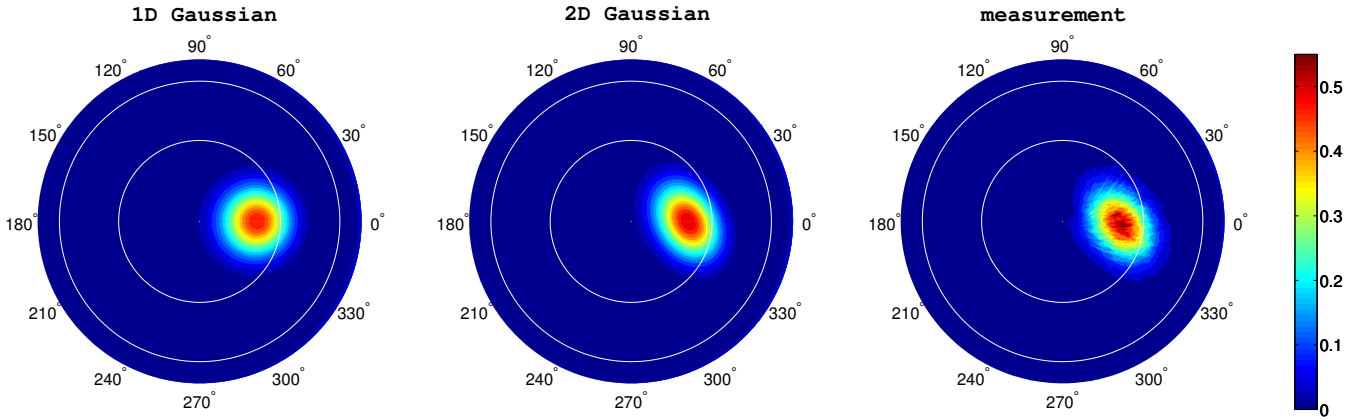

Figure 1: Comparison of reflectances for model simulations assuming a 1-D Gaussian BRDF (left), a 2-D Gaussian BRDF (middle), and measurements (right).

Use of
(1) a 2-D Gaussian surface slope distribution for singly scattered light, and
(2) a 1-D Gaussian surface slope distribution for multiply scattered light
is quite successful because the **2-D BRDF simulates the sunglint** very well, while the **1-D BRDF is sufficient to simulate the sky reflectance**.

3. Standard ocean color algorithms do not work well in coastal areas

Below (lower panels) is an example of the problem caused by the infamous **negative** water-leaving radiance problem due to failure of the atmospheric correction.

- Can the failing atmospheric correction be fixed? Or can it be
- alleviated by using **simultaneous atmosphere/ocean retrievals** based on an RT model for the coupled atmosphere/ocean system (upper panels)?

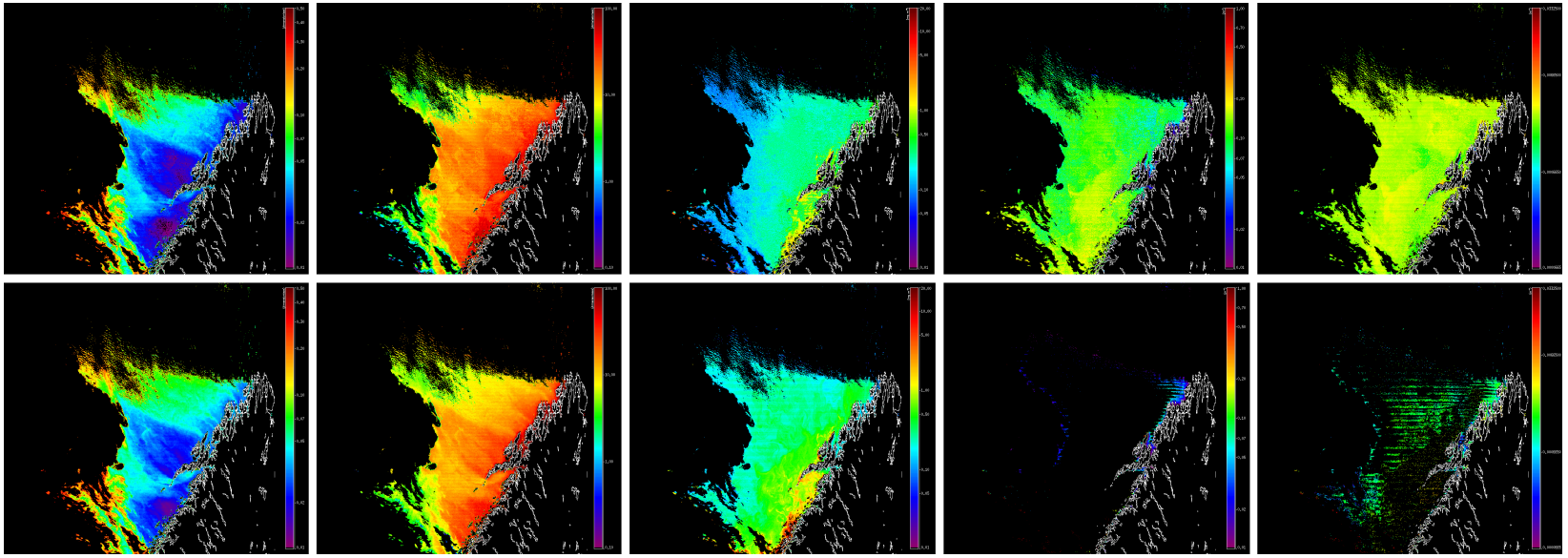

Comparison between **simultaneous** (OC-SMART, top) and **standard** (SeaDAS, bottom) retrievals for a MODIS image on 04/18/2014 over a coastal area in northern part of Norway. From left to right: τ_{869}, f, CHL, CDOM and b_{bp}, respectively.

Final thought: What about using vector (polarized) RT simulations?

- Preliminary results* indicate that even for **radiance-only** measurements:
- **the accuracy of the retrievals could be improved by using a vector (polarized) forward RT model to compute the radiances used in the inversion step.**

Hence, for ocean color retrievals from geostationary platforms, we should explore the advantage of using:

1. the pseudo-spherical approximation combined with
   - polarized (vector) radiative transfer simulations,
   - a 2-D Gaussian distribution of surface slopes,
2. neural networks and optimal estimation for:
   - simultaneous retrieval of atmospheric and marine parameters, and
   - assessments of retrieval accuracy and error budgets.

*Stamnes, S., Y. Fan, N. Chen, W. Li, T. Tanikawa, Z. Lin, X. Liu, S. Burton, A. Omar, J. J. Stamnes, B. Cairns, and K. Stamnes, Advantages of measuring the Q Stokes parameter in addition to the total radiance I in the detection of absorbing aerosols, Front. Earth Sci., 6:34, 2018.

Next: Practice Example

Simulated RGB Pixels Examples (1)

Practice with AccuRT – simulate the color of the ocean

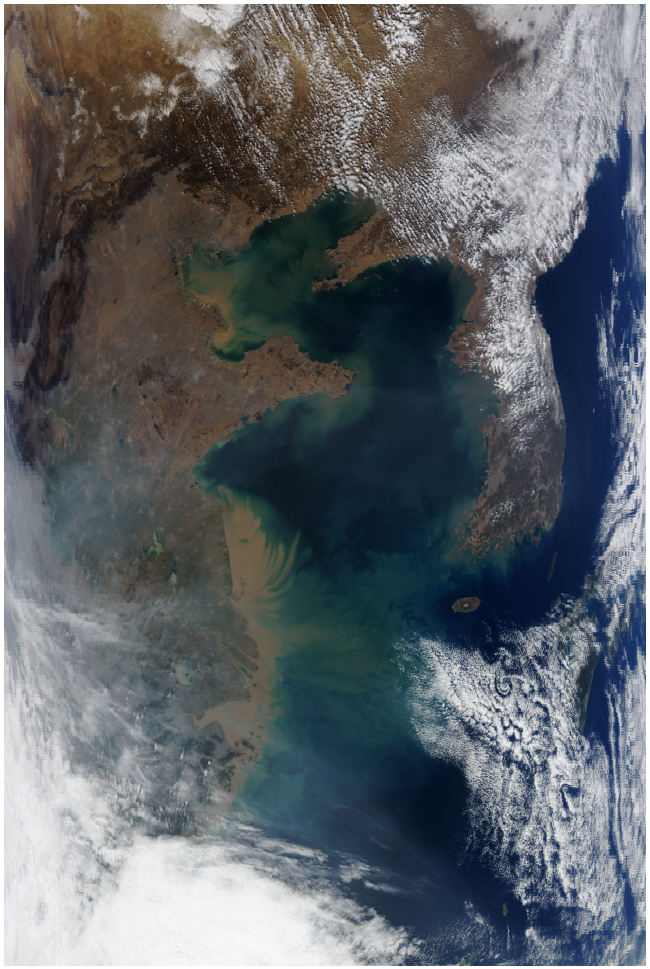

Aqua MODIS RGB 03/10/2011

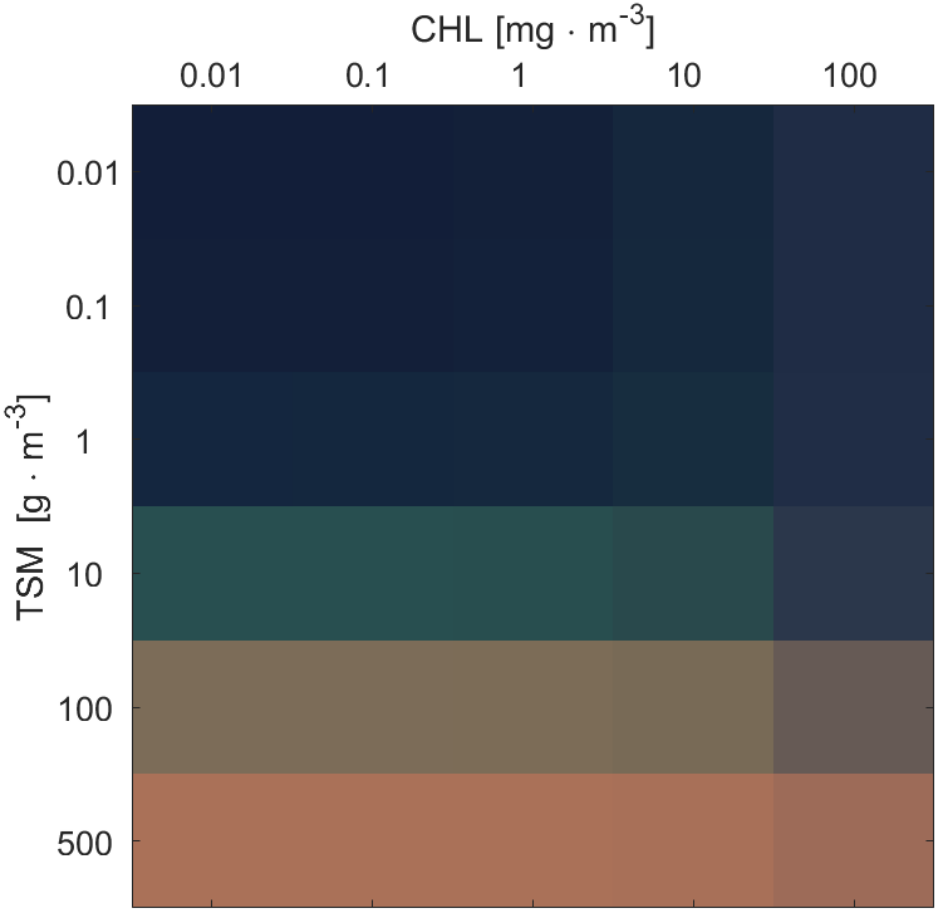

AccuRT simulated RGB pixels
(Solz=40°,Senz=10°, Relaz=120°)

Simulated RGB Pixels Examples (2)

Practice with AccuRT – simulate the color of the ocean

AccuRT configuration file for the simulation:

- Main configuration file: ocsim
- Ocean configuration file: /ocsimMaterials/water_impurity_ccrr, chl.txt, tsm.txt
- Aerosol configuration file: /ocsimMaterials/aerosol

Tag setting in 'ocsim' (all other tags use default values):

- SOURCE_TYPE = constant_one
- SOURCE_ZENITH_ANGLE = 40
- STREAM_UPPER_SLAB_SIZE = 40
- MATERIALS_INCLUDED_UPPER_SLAB = earth_atmospheric_gases aerosols
- MATERIALS_INCLUDED_LOWER_SLAB = pure_water water_impurity_ccrr
- DETECTOR_AZIMUTH_ANGLES = 120
- DETECTOR_POLAR_ANGLES = 10
- DETECTOR_WAVELENGTHS = 469 555 645
- SAVE_RADIANCE = true
- REPEATED_RUN_SIZE = 30

Tag setting in 'water_impurity_ccrr' :

- CHLOROPHYLL_CONCENTRATION = chl.txt
- MINERAL_CONCENTRATION = tsm.txt
- CDOM_ABSORPTION_443 = 1 0.1

Tag setting in 'aerosol' :

- FINE_MODE_FRACTION = 0.4
- RELATIVE_HUMIDITY = 0.7

MATLAB script for data preparation and image plotting:

- ocparam.m creates 'chl.txt' and 'tsm.txt'
- plot_RGB_OC.m reads the simulation data and plots the RGB image.